**From St. Erik's Eye Hospital,
Karolinska Institutet, Stockholm, Sweden**

ULTRAVIOLET RADIATION AND CORNEA

Alexander Podskochy

Stockholm 2002

Published and printed by Karolinska University Press
Box 200, SE-171 77 Stockholm, Sweden

ISBN 91-7349-118-7

To my parents

ABSTRACT

Background. Acute exposure of the mammalian eye to UVR results in development of photokeratitis after a period of a few hours. Chronic exposure to UVR is associated with an increased risk of several corneal disorders, including pterygium, climatic droplet keratopathy, and climatic proteoglycan stromal keratopathy. The proteoglycan content in these pathological conditions is altered. The mechanisms, leading to the corneal damage after UVR exposure, are not fully known. In the present work the action of different UVR wavelengths and doses on the rabbit cornea was studied. The mechanisms of the corneal cell death after UVR exposure, and the influence of UVR induced keratitis on the corneal proteoglycans, specifically hyaluronan and biglycan, have been investigated. An experimental model to study the chronic UVR exposures has been characterised.

Methods. New Zealand rabbit eyes were exposed to single or repeated UVR doses. UVR wavelengths of 270, 280, 290, and 310 nm were used at doses producing photokeratitis, and at subthreshold doses. Immunohistochemical methods were used to detect hyaluronan (HA), apoptosis, and Fas ligand protein in the corneal specimens. The morphology of the corneas was studied using light and transmission electron microscopy. Expression of the biglycan gene was evaluated by RT-PCR technique.

Results. UVR at subthreshold doses did not produce any corneal damage that could be detected in the light microscope. Apoptosis was detected to be one important mechanism leading to corneal cell damage after UVR exposure at photokeratitis doses. Photokeratitis doses at 270, 280, and 290 nm led to a superficial corneal damage. Apoptotic cells were found only in the epithelial layer and superficial keratocytes. UVR exposure at photokeratitis doses at 310 nm resulted in severe corneal damage, where apoptosis was seen in the epithelium, the

keratocytes through the whole corneal stromal thickness, and the endothelium. During the first seventy-six hours after exposure to 310 nm UVR at photokeratitis doses, keratocytes underwent apoptosis and disappeared. Keratocytes bordering this damaged cell-free area started to produce hyaluronan during the repopulation phase. The production of hyaluronan peaked at 7 days after UVR exposure. Fourteen days after exposure the corneas were completely restored, and only trace amounts of hyaluronan was detected close to the Descemet's membrane. Repeated exposures of the corneas to photokeratitis doses at 310 nm at 1 week intervals resulted in hyaluronan deposits in the corneal stroma, and reduction of the keratocyte apoptosis level.

Fas ligand protein in the normal rabbit corneas was expressed only in epithelial and endothelial cells. UVR exposure of the corneas at photokeratitis doses resulted in Fas ligand protein expression also in keratocytes, suggesting the Fas/Fas ligand system activation leading to apoptosis.

Biglycan gene was not expressed in the normal rabbit corneas. However, UVR exposure at photokeratitis doses activated a distinct biglycan gene expression at 7 days after exposure. Biglycan gene expression decreased 28 days after exposure.

Conclusion. A photokeratitis dose of 310 nm UVR is needed to cause a significant keratocyte damage. A photokeratitis dose of the shorter wavelengths causes damage to epithelial cells and superficial keratocytes only, due to a very high absorption of these wavelengths in the epithelium. The keratocyte production of HA appears to be a sign of cell readiness to repopulate the damaged stroma devoid of keratocytes. Apoptosis, initiated by Fas/Fas ligand system activation, is a mechanism leading to the corneal cell death after UVR exposure. Repeated UVR exposures lead to increased production and accumulation of HA in the corneal stroma. The repopulated keratocytes are

much more resistant to apoptosis than the native ones. HA accumulation may be a sign of long term changes in the cornea, leading to corneal degeneration. There is no expression of biglycan gene in the normal rabbit cornea. The UVR exposure leads to a strong expression of biglycan gene in the rabbit cornea that decreases 4 weeks after exposure indicating the biglycan involvement in the corneal repair process. Biglycan appears to be a novel marker of the corneal wound healing.

Key words. Cornea, UVR, keratocytes, apoptosis, Fas ligand, hyaluronan, biglycan, rabbit, wound healing.

LIST OF PAPERS

This thesis is based on the following papers, which are referred to by their Roman numerals:

I. Podskochy A, Fagerholm P. Cellular response and reactive hyaluronan production in UV-exposed rabbit corneas. ***Cornea***. 1998;17:640-645.

II. Podskochy A, Gan L, Fagerholm P. Apoptosis in UV-exposed rabbit corneas. ***Cornea***. 2000;19:99-103.

III. Podskochy A, Fagerholm P. The expression of Fas ligand protein in ultraviolet-exposed rabbit corneas. ***Cornea***. 2002;21:91-94.

IV. Podskochy A, Fagerholm P. Repeated UVR exposures cause keratocyte resistance to apoptosis and hyaluronan accumulation in the rabbit cornea. ***Acta Ophthalmologica Scandinavica***. 2001;79:603-608.

V. Podskochy A, Koulikovska M, Fagerholm P, van der Ploeg I. Biglycan gene expression in UV-exposed rabbit corneas. ***Submitted manuscript***.

Reprints were made with kind permission from the publishers.

CONTENTS

LIST OF ABBREVIATIONS

ABC	Avidin-Biotin-Complex
ARVO	Association for Research in Vision and Ophthalmology
CIE	Commission Internationale de l'Éclairage (International Lighting Commission)
cDNA	Complementary deoxyribonucleic acid
DNA	Deoxyribonucleic acid
ECM	Extracellular matrix
EGF	Epidermal growth factor
Excimer	Excited dimer
FGF	Fibroblast growth factor
FN	Fibronectin
GAG	Glycosaminoglycan
GAPDH	Glyceraldehyde phosphate dehydrogenase
HA	Hyaluronan
HABP-R	Hyaluronan binding proteoglycan region
Hc	Threshold dose of ultraviolet radiation to produce keratitis
HGF	Hepatocyte growth factor
IL	Interleukin
KGF	Keratinocyte growth factor
LASIK	Laser in situ keratomileusis
MMP	Matrix metalloproteinase
mRNA	Messenger ribonucleic acid
O	Oxygen
PBS	Phosphate-buffered saline
PDGF	Platelet-derived growth factor
PMNs	Polymorphonuclear leukocytes

PRK	Photorefractive keratectomy
RT-PCR	Reverse transcriptase-polymerase chain reaction
TEM	Transmission electron microscopy
TGF	Transforming growth factor
TIMP	Tissue inhibitor metalloproteinase
TNF	Tumor necrosis factor
TUNEL	Terminal deoxynucleotidyl transferases (TdT)-mediated dUTP-digoxigenin nick end labeling
UVR	Ultraviolet radiation

1. INTRODUCTION

1.1 Development of the cornea

The cornea develops from the interaction of the surface ectoderm and the neural crest derived mesenchyme.[1-3] The surface ectoderm which seals over the lens pit, forms the future corneal epithelium. The mesenchymal cells give rise to the deeper layers of the cornea including Bowman's layer, stroma, endothelium, and Descemet's membrane.

1.2 Corneal anatomy and physiology

The cornea is the gateway of light to project external images on the retina. The surface of the cornea is responsible for most of the refraction of the eye.[4] The transparency of the cornea is a very important property. Corneal transparency is a result of interaction of a number of related factors, such as smoothness and regularity of the epithelium, corneal avascularity, and the regular arrangement of the cellular and extracellular components in the stroma.[5-11] Due to a highly exposed position, the cornea also constitutes a barrier to trauma and infection.

The human cornea is composed of five layers: epithelium, Bowman's layer, stroma, Descemet's membrane, and endothelium (Figure 1). The corneal epithelium is a stratified, squamous nonkeratinized epithelium. In humans, the thickness of the epithelium is about 50-60 μm. The adjacent cells are held together by numerous desmosomes and to the underlying basal lamina by hemidesmosomes and anchoring filaments.[12,13] New cells are derived from mitotic activity in the limbal stem cells and in the basal cell layer.[14,15]

The Bowman's layer, or anterior limiting lamina, is a modified acellular region of the anterior stroma and consists of randomly arranged collagen fibers (type I,II,V and VI).[16-18] The thickness of the Bowman's layer in humans is about 8-12 μm. Rabbits are lacking the Bowman's layer.

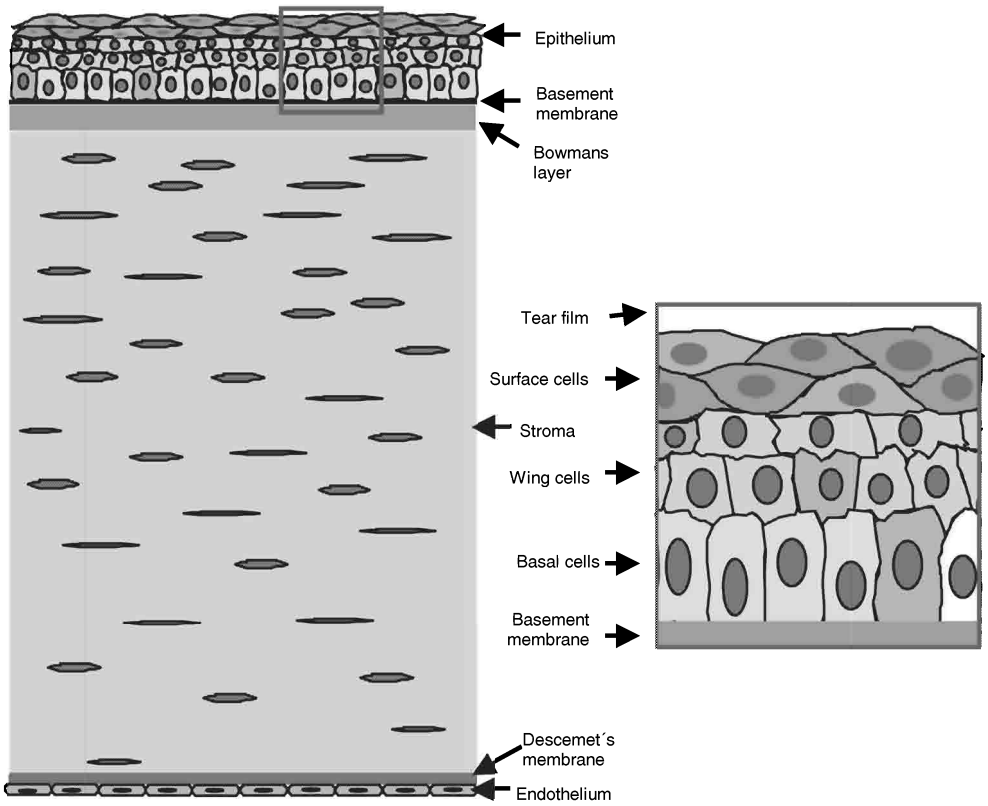

Figure 1. Structure of normal human cornea.

The corneal stroma is a tissue with a remarkable regularity. It is the thickest corneal layer (400-500 μm) and consists of collagen lamellae that are oriented parallel to the corneal surface.[19] Extremely flattened cells of mesenchymal origin, called keratocytes, lie between the corneal lamellae. They are highly specialised and become activated after trauma. Keratocytes are stellate in shape with thin cytoplasmic extensions, containing only a very small number of organelles. The collagen lamellae are highly organised, where the adjacent lamellae are oriented at right angles, with the exception of the anterior third part of the stroma in which the lamellae display a more oblique orientation.[20] The collagen type I predominates,

but types III, V, and VI are also present.[21-23] The extracellular glycosaminoglycans (GAG) and proteoglycans form bridges between the collagen fibers, that regulates the highly regular spacing of the collagen in the lamellae.[24-27] The organisation of the lamellae and the extracellular matrix (ECM) is the key to the corneal transparency.

The Descemet's membrane, or posterior limiting lamina, is placed between the posterior stroma and endothelium, and is about 8-12 μm thick. Descemet's membrane represents a modified basement membrane of the corneal endothelium.

The corneal endothelium is a single layer of flat cells of mesenchymal origin on the posterior surface of the cornea. It has a critical role in maintaining corneal hydration and thus transparency.[28,29] The endothelial cells in the human cornea have a very low regenerative capacity. Lost endothelial cells are replaced by spreading and enlargement of adjacent cells.[30,31] However, endothelial cells in rabbit can regenerate, and lost cells can be replaced by new cells.[32-34]

The cornea is richly supplied by sensory nerves derived from the ophthalmic division of the trigeminal nerve, via the long ciliary nerves.

The cornea is nourished by diffusion from the aqueous humor in the anterior chamber of the eye, from the vascular structures in the limbus, and from the tears.

1.3 Extracellular matrix of the corneal stroma

The major corneal glycosaminoglycan (GAG) is keratan sulfate.[35-40] The nonsulfated chondroitin is also present in the central cornea, while towards the periphery dermatan sulfate is the second major GAG.[41,42] The corneal stroma is unusual in that it contains no hyaluronic acid, or hyaluronan (HA), except at the limbus where there is a gradual increase in concentration towards the sclera.[43-46] However, reactive formation of HA has been described following

different models of corneal wounds, such as excimer laser surgery,[47] alkali wounding to the cornea,[48] and mechanical wounding (knife incision).[49,50] HA deposits can bee found in the diseased corneas with keratoconus, bullous keratopathy, Fuchs dystrophy, corneal degenerations etc.[51]

Corneal GAGs in the native state bind the protein component and form proteoglycans. In recent years the proteins of the major proteoglycans of the corneal stroma have been identified and their genes cloned. Keratan sulfate proteoglycans consist of three unique proteins, each modified with keratan sulfate chains and each a product of a separate gene.[52] Dermatan sulfate proteoglycan proteins are coded by two related genes. Decorin is the predominant dermatan sulfate proteoglycan protein in the corneal stroma.[53] Another dermatan sulfate proteoglycan protein, biglycan, has been identified in the epithelium of the normal human cornea, and in very small amounts in the stroma.[53,54] The stromal deposition of biglycan has been described in pathological conditions of the cornea, such as keratoconus, bullous keratopathy and corneal scars.[55,56] The keratan sulfate proteoglycan proteins, contrary to the dermatan sulfate proteoglycans, are present in pathological corneal stroma in amounts comparable with those in normal stroma.[57]

The critical region in proteoglycans is their linkage sites. For keratan sulfate the link is an N-glycosidic bond between N-acetyl glucosamine and asparagine in the core protein. Dermatan sulfate contains xylose residues at its terminal site. Both keratan sulfate and dermatan sulfate proteoglycans bind to the collagen fibers at specific binding sites, suggesting that these sites are essential to the spacing of the fibers. Keratan sulfate proteoglycans appear to bind to the step region of the fibers while dermatan sulfate proteoglycans bind to the gap.[58]

Proteoglycans play an important role in chemical signalling

between cells. They bind various signalling molecules such as certain growth factors. Such binding can enhance or inhibit the activity of the growth factor. Fibroblast growth factor (FGF), for example, which stimulates the corneal cells to proliferate, binds to heparan sulfate chains of proteoglycans.[59,60] Whereas in most cases the signalling molecules bind to GAG chains of the proteoglycan, this is not always so. Transforming growth factor beta (TGF-β) binds to the core protein of proteoglycan decorin.[59,60] Binding to decorin inhibits the activity of the TGF-β. Proteoglycans also bind and regulate the activities of other types of secreted proteins, such as proteolytic enzymes (proteases) and protease inhibitors. Binding to a proteoglycan could control the activity of a protein in any of the following ways: (1) it could immobilize the protein close to the site where it is produced, thereby restricting its range of action; (2) it could sterically block the activity of the protein; (3) it could provide a reservoir of the protein for delayed release; (4) it could protect the protein from proteolytic degradation, thereby prolonging its action; and (5) it could alter or concentrate the protein for more effective presentation to cell-surface receptors.[61,62] Proteoglycans are thought to act in all these ways to help regulate the activities of secreted proteins.

1.4 General aspects on corneal wound healing

Corneal wound healing has been excessively studied during the last decades using the alkali burn and excimer laser wound models as well as other models. The complex process of wound healing may be simplified by dividing the sequence of events into three phases: inflammatory, proliferative, and remodelling phases.[63]

The inflammatory phase is characterised by the influx of leukocytes and monocytes to the wound area, followed by lymphocytes and macrophages, and the release of a variety of growth factors and other molecules. Leukocytes,

especially polymorphonuclear leukocytes (PMNs), enter the open wound from the tear film or penetrate into the wound through the corneal stroma.[64,65] PMNs arrive first to the wound and monocytes some days later.[65] Monocytes possess the potential to turn into macrophages. Leukocytes and macrophages clean the wound from debris and bacteria and liberate interleukins and growth factors. These cytokines promote migration and proliferation as well as the synthesis of new extracellular matrix and collagens. Leukocytes disappear from the wound when the epithelial coverage has been completed.

In corneal alkali burns, products liberated by PMNs, such as collagenases, are responsible for the devastating effects that may lead to corneal ulceration. If PMNs are prevented from entering the cornea from the tear film after alkali burns by applying glued-on contact lenses, stromal ulceration is greatly diminished.[66] Furthermore, the prevention of leukocytes from entering the wounded area in alkali burns, by blocking the PMNs adhesion to the vascular vessels through the intravenous administration of fucoidin, retarded the epithelial healing rate.[65] This suggests that PMNs play a role in promoting the epithelial healing, probably via the liberation of cytokines, such as TGF-β.

Cytokines are hormone-like proteins that serve as principal mediators of immunological and inflammatory responses. Cytokines can act on the cells in which they are produced (autocrine function), on the surrounding cells (paracrine function), and on the so called goal-cells located in other tissues (endocrine function). Interleukins and growth factors are the most important cytokines that are thought to be involved in the corneal wound healing.

It is not only leukocytes that may produce cytokines. For example, injured corneal epithelial cells can release interleukin-1 (IL-1) and interleukin-6 (IL-6). IL-1, in turn, is capable to trigger apoptosis of underlying keratocytes in the

corneal stroma through activation of Fas/Fas ligand system.[176,177] IL-6 promotes collagen I synthesis and modulates matrix metalloproteinase-2 (MMP2).[67]

Other cytokines, such as TGF-β, FGF, epidermal growth factor (EGF), and others may play a role in communication between cells that regulate the wound healing process. TGF-β inhibits mitosis and promotes epithelial migration.[68,69] This action is facilitated by fibronectin (FN) and tumor necrosis factor alpha (TNF-α). Furthermore, TGF-β stimulates the synthesis of extracellular matrix components, contributing to scar formation. Antibodies against TGF-β have been successfully used to reduce scar tissue in the skin and have been applied to the cornea after photorefractive keratectomy, reducing haze formation.[70,71] EGF stimulates DNA synthesis, proliferation and differentiation of epithelial cells.[69] Hepatocyte growth factor (HGF) can also promote epithelial migration and proliferation.[72] Platelet-derived growth factor (PDGF) facilitates the activity of HGF in epithelial migration and stimulates synthesis of extracellular matrix.[73] Keratocytes synthesise keratinocyte growth factor (KGF), which stimulates epithelial cell proliferation.[74] Production of a number of cytokines, such as IL-1, IL-6, IL-8, and TNF-α has been documented after UVR exposure.[75]

During the proliferative phase of corneal wound healing, re-epithelialisation occur as well as migration of keratocytes, and also the production of the provisional extracellular matrix. The migration of the epithelium is preceded by the cease of the mitosis at the edges of the wound. This latent phase lasts about 8 hours. During this phase the hemidesmosomal attachments between the basal cells and basement membrane disappear from the wound edge.[76] Superficial cells are liberated and the formation of lamellopodia and filopodia marks the beginning of the migration.[77] Also, cells increase their size and

cover a larger area. Actin filaments are assembled in the basal region of the cells, facilitating their movements. At the same time as the migrating front of epithelial cells moves towards the centre of the wound, these cells synthesise structural proteins over the denuded stroma to facilitate migration. A new basement membrane is formed under the migrating cells and new hemidesmosomes are re-established from the periphery to the centre of the wound.[78]

As it has been mentioned earlier, the epithelial injury may in turn trigger apoptosis of underlying keratocytes through release of IL-1 and Fas/Fas ligand system activation.[176,177] The traumatic agents may also lead to destruction of stromal extracellular matrix. The injury and the subsequent apoptosis cause a cell-free area in the corneal stroma. Keratocytes in the border to this cell-free area become activated. The activated keratocytes start to produce new collagen fibrils and extracellular matrix components.[79] Hyaluronan, that is not normally present in the corneal stroma, is produced by activated keratocytes during this repopulation phase of wound healing. Hyaluronan is thought to facilitate migration and repopulation of the cell-free area in the stroma by keratocytes.[47,48]

The remodelling phase of corneal wound healing consists of wound contraction, extracellular matrix deposition, degradation and modification. This phase can last for several months and even years. Wound contraction is mediated by the myofibroblasts transformed from keratocytes by TGF-β.[80] Enzymes, such as matrix metalloproteinases act in the remodelling of the healing tissue. These enzymes are modulated by tissue-inhibitor metalloproteinases (TIMPs) and by TGF-β, guarding excessive breakdown of the extracellular matrix.[81]

1.5 Ultraviolet radiation

By CIE (Commission Internationale de l'Éclairage) definition, optical radiation between 100 and 400 nm is

considered as ultraviolet radiation (UVR).[82] UVR can be divided in three regions: UVR-C with wavelengths between 100 and 280 nm, and with photon energy 4.4-12.4 eV; UVR-B between 280 and 315 nm with photon energy 3.9-4.4 eV; and, finally, UVR-A between 315 and 400 nm with photon energy 3.1-3.9 eV.

Man is exposed to the highly toxic UVR-C only from artificial sources, because UVR-C from the solar radiation is completely absorbed by atmosphere and does not reach the earth. However, solar UVR-B and UVR-A penetrate the atmosphere and reach the earth surface. The irradiance of the solar radiation on the earth depends on several factors such as latitude, altitude, season and solar elevation angle; concentrations of smoke and particles from large forest fires and volcano eruptions, that alter the absorption properties of the atmosphere; and concentrations of ozone in the stratosphere. Ozone is formed in the stratosphere due to the absorption of short-wave solar radiation (140-200 nm) by oxygen. The ozone in turn absorbs longer solar radiation with wavelengths between 200 and 300 nm, and is split into oxygen, again.[83] However, the stratospheric ozone influence upon the solar spectrum is most prominent around 300 nm.[84]

Increased sun exposure (vacations in southern latitudes, skiing in mountains, sun tanning etc.) in combination with a longer life-expectancy has increased the amount of natural ultraviolet radiation exposure that people receive in their lifetime.[85-87] The changes in the atmosphere and the ozone layer that allow a greater amount of UVR with shorter wavelengths to reach the earth, enhance this exposure.[88,89] Artificial sources of UVR are used very widely in sun tanning and for industrial needs, e.g., sterilisation, welding arcs, lasers etc. However, the most affected group in Sweden is probably skiers who fail to wear protective goggles, that leads to prolonged exposure to UVR reflec-

ted from snow. Snow is essentially the only material found in the natural environment with a high reflectance (approximately 88%) in the UVR-B region.[90,91] Eskimos who have had to live with this environmental situation have evolved a type of eye protection using whale bone with slits cut into it to provide a highly restricted field of view which eliminates reflected UVR from nearby snow and still permits viewing of distant objects.[90] The second natural material with high reflectance is sand on the beaches and in the desert areas. The reflectance of the dry sand in the UVR-B region is approximately 17%.[90,91] Water reflects very little and transmits a large percentage.

1.6 Radiometric terminology

The effects of optical radiation upon any biological structure are not dependent directly upon the incident power in watts (W) or energy in joules (J), but upon the concentration of power or energy per unit area and the time of exposure. The quantity which describes "dose rate" is ***irradiance*** with units of W/cm^2 or W/m^2. The ***dose*** or ***radiant exposure*** is the irradiance per time unit, and is measured in J/cm^2 or J/m^2.

1.7 General aspects on photochemistry and photobiology

Most photobiological effects, including vision, are fundamentally (at least initially) a photochemical process. Photochemical reactions can also induce cell damage, either directly or indirectly. When the absorbing chromophore, or molecule that absorbs radiation, is chemically changed during the reaction to a toxic molecule, the reaction is called a direct photochemical reaction. When the absorbing chromophore does not change chemically itself, but causes a chemical change in another, neighbouring, molecule that becomes toxic, the reaction is called a photosensitised reaction. A molecule, that absorbs a photon and enters a higher, unstable, energy level, or excited state, is called

photosensitiser. There are two principle pathways for the photosensitiser to act.[92] The first pathway, or radical pathway, is activated when the photosensitiser interacts with the target molecule through formation of free radicals. The second pathway is the singlet oxygen pathway, when the photosensitiser interacts with oxygen in the tissues with formation of reactive oxygen species (ROS), such as singlet oxygen, which in turn induce chemical changes in the target molecule.

Direct photochemical reactions and photosensitised reactions can lead to enzyme inactivation, cellular membrane damage through lipid peroxidation, protein aggregation, and DNA alteration.[93-98] Enzymatic inactivation may result in decreased cellular metabolism and lead to decreased synthesis of membrane proteins and cellular edema.[99-103] Lipid peroxidation of cellular membranes may lead to an increased membrane permeability that, in turn, results in cellular edema.[104-107] Damage to DNA may lead to formation of strand breaks and photoproducts.[108-112] Formation of photoproducts has been associated with cancerogenesis.[113-116]

For most photochemical and photobiological processes, UVR at short-wave region is normally more effective than longer wavelengths, because the energy per photon is inversely proportional to the wavelength.

The amount of UVR that is absorbed by the tissue and the subsequent damage depends, in general, on the concentration of chromophores that this tissue contains. Different chromophores have individual preferential absorption wavebands that modulates the susceptibility of different tissues to UVR. Proteins and aromatic amino acids, especially tryptophan, are the most important chromophores in cornea.[117,118] Tryptophan absorbs more than 95% of UVR-B. Another important chromophore in cornea is ascorbate (vitamin C), that has its highest concentration in the epithelium.[119]

The cornea has developed a number of protective systems that prevent or reduce the damage to the eye from UVR and other oxidative stresses. Glutathione, ascorbate, α-tocopherol (vitamin E), superoxide dismutase, lactoferrin and catalase are main physiological anti-oxidative agents protecting the eye against UVR by their scavenging activity.[120-128]

1.8 UVR action spectrum for the cornea

The action spectrum for corneal damage after UVR has been set from 210 to 315 nm (Figure 2).[129] UVR in the range from 320 nm to 400 nm are not considered part of the action spectrum of the cornea because the energy levels of UVR exposure necessary to produce minimal damage in this range are very high. For example, the threshold exposure level at 315 nm is 450 times the corneal threshold level at 270 nm.[130] UVR at 270 nm is considered as most effective in producing corneal damage. Primate and human corneas are more sensitive to UVR than rabbit corneas as shown in Figure 2.

1.9 Absorption of UVR by the cornea

Cornea absorbs most of UVR below 300 nm, and the corneal epithelium stands for the biggest part of this absorption.[131] Due to this absorption pattern, the corneal epithelium protects deeper lying eye structures from UVR damage in the range below 300 nm. However, approximately a half of UVR energy that is absorbed by the cornea in the region above 300 nm, is absorbed by the corneal stroma (Figure 3).

UVR absorption by other ocular media is shown in Table 1.

UVR range	Cornea	Anterior chamber	Lens	Vitreous
<280 nm	100	-	-	-
300 nm	92	6	2	-
320 nm	47	16	36	1
340 nm	37	14	48	1
360 nm	32	14	52	2

Table 1. Absorption of UVR by different ocular media (From Boettner & Wolter, 1962).[132] Numbers are the percentages of absorbed radiation by ocular media.

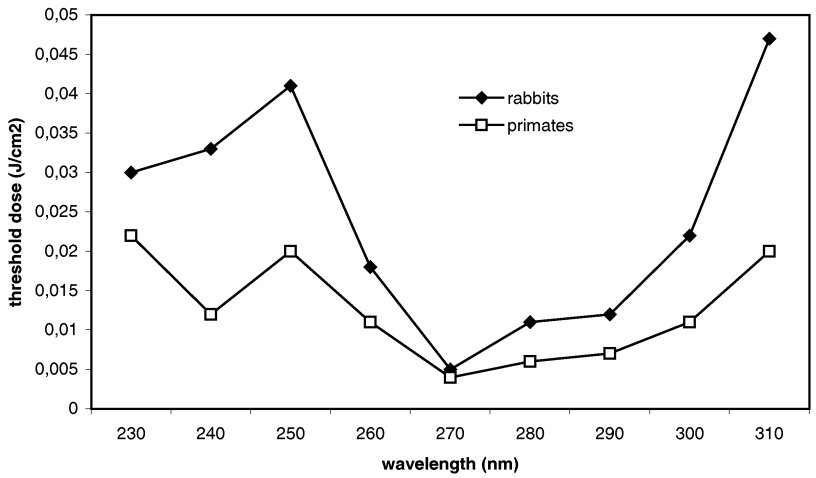

Figure 2. Comparison of the corneal action spectrum in the 230 nm to 310 nm wavelengths range for rabbits and primates (From Pitts et al, 1971).

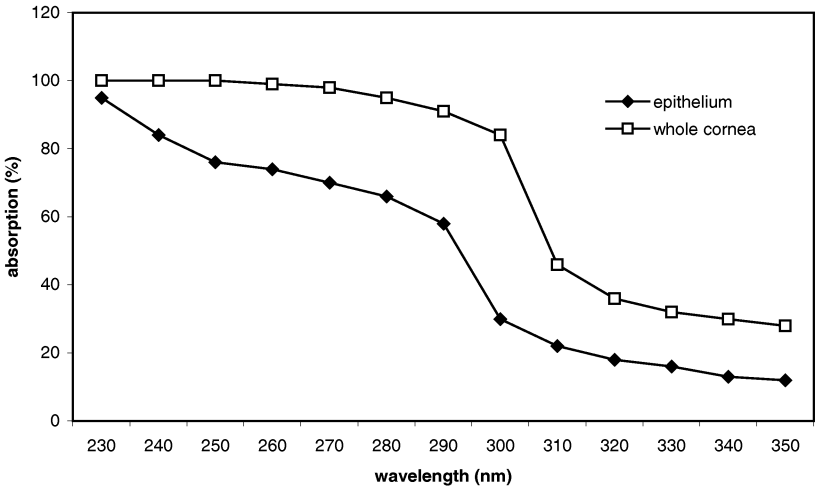

Figure 3. Absorption of UVR by the cornea (From Kinsey, 1948).

1.10 Oxygen dependence of corneal exposures

Zuclich & Kurlich[133] have shown that the UVR-A exposure thresholds for cornea were oxygen dependent. Using the argon laser emitting UVR at 351.1 nm and 363.8 nm, they found that the threshold level to produce corneal damage in the eyes flushed with air was 82 J/cm^2, while oxygen flushed eyes had threshold at 66 J/cm^2. The nitrogen flushed eyes had the threshold at 133 J/cm^2. This means that the more oxygen in the tissue the more severe corneal damage can be expected.

1.11 Acute UVR exposure of the cornea

The condition of the cornea after an acute exposure to UVR is called "keratoconjunctivitis photoelectrica", or "photo-ophthalmia", or "photokeratitis". An acute UVR exposure is usually followed by a latency period, the extent of which depends of the intensity of the exposure but is typically 6-12 hours.[134-136] The anterior

part of the eye, the eyelids and the skin surrounding the eyes becomes reddened. There is a sensation of a foreign body or "sand" in the eyes, and the affected person becomes very sensitive to light (photophobia). This is accompanied by excess tear production (lacrimation) and closure of the lids to avoid pain (blepharospasm). If evaluated in the slit lamp microscope, the affected eye may reveal conjunctival injection, debris, epithelial swelling, erosions and corneal edema. These acute symptoms last usually from 6 to 24 hours but almost all discomfort disappears within 48 hours.

1.12 Chronic UVR exposure of the cornea

The chronic exposure to sunlight, specifically to UVR, is associated with an increased risk of several corneal disorders, including pterygium, climatic droplet keratopathy, and climatic proteoglycan stromal keratopathy.

Pterygium occurs more commonly in tropical or sunny areas and has been ascribed to greater sun exposure, specifically to UVR-B.[137,138] Pterygium is a wing-shaped extension of the conjunctiva consisting of fibrovascular tissue that invades the superficial cornea. The pathologic changes in pterygium consist of elastoid degeneration of collagen and the appearance of subepithelial fibrovascular tissue.[139-141] The cornea shows destruction of Bowman's layer. The epithelium may be normal, thick, or thin and may occasionally show dysplasia. Mild inflammatory changes are often present. Pterygium not seldom impairs the vision.

Climatic droplet keratopathy is relatively unusual and more often reported in harsh climates, such as arctic or desert areas.[142] Ultraviolet radiation is thought to play a role in its etiology.[138,143-146] This condition has been reported under different names, including corneal elastosis, keratinoid degeneration, spheroidal degeneration, Bietti's nodular dystrophy, proteinaceous degeneration, and Labrador

keratopathy. All cases show extracellular deposits of amino acids.[145-147] This condition is often bilateral and more common in males.[148-155] It is characterized by the formation of grey or yellow-brown, drop-like deposits superficially within the interpalpebral fissure. The initial deposits are usually found near the limbus. The "droplets" involve Bowman's layer and the superficial corneal stroma, as well as the subepithelial conjunctiva.[156-158] With time, the deposits coalesce and enlarge, infiltrate the anterior one third of the stroma and spread across the cornea in a band-shaped pattern. Vision is impaired gradually. In severe cases keratoplasty may be necessary.

Climatic proteoglycan stromal keratopathy is a corneal degeneration recently described in the Middle East by Waring et al.[159] This corneal degeneration is also thought to be associated with chronic UVR. Its pathological substrate is deposition of proteoglycans that lead to corneal haziness. This condition is confined to the interpalpebral fissure in a band-shaped pattern, and may be accompanied by other disorders that are associated with climatic exposure, such as climatic droplet keratopathy and mild calcific band keratopathy. The major criterion for diagnosis of this corneal condition is a central, horizontally oval or round, grey stromal haze that is usually more extensive anteriorly with a tapering edge, and smaller posteriorly. The experienced Middle Eastern ophthalmologists indicate that this condition is very frequent in their countries, and because of that it is often overlooked and not recorded.[159] This condition very rarely leads to severe vision impairment, but in some cases keratoplasty is needed.

1.13 Aims of the study

The mechanisms of cell death in the cornea after UVR exposure are not fully known. There is also a lack of information about the pathophysiology of the corneal extracellular matrix components. The latter probably play a role in UVR associated corneal degenerations. These questions in combination with the increased use of UVR in the every day life gave the motive for the present study.

The specific aims of the study were:

- To study the cellular response and hyaluronan production in the cornea after exposures to different UVR wavelengths and doses.
- To investigate if apoptosis could be a mechanism of corneal cell death after UVR exposure.
- To study the expression of Fas ligand protein in the cornea after UVR exposure.
- To examine the effects of repeated UVR exposures on keratocyte apoptosis and HA production in the cornea.
- To study the expression of biglycan gene in the cornea after UVR exposure.

2. MATERIALS AND METHODS

2.1 Sources of ultraviolet radiation

Paper I

The ultraviolet source used was an 150-W xenon mercury high-pressure lamp, powered by spectral energy ultra-stable power supply. The lamp was mounted in a lamphousing LH150. The radiation from the source was focused at the monochromator entrance slit by the housing optics (Figure 4). The exit optical beam was focused by a quartz lens producing a beam size of approximately 3x6 mm^2 at the center of the rabbit cornea (Figure 5). An 8 nm waveband was obtained with a double-grating monochromator for all wavelengths used in the experiment, i.e. 270, 290 and 310 nm. Entrance and exit slits were set to pass a nominal full band-pass of 8 nm. The spectral distribution for each monochromator set-up was measured with an optical spectroradiometer (Optronic 742) without the focusing exit lens. It was not possible to measure the exposure beam in the same focus area as used during the rabbit exposures due to overloading of the spectroradiometer. Instead the relative spectral distribution was regarded to be constant and measured further away in the beam. The absolute level was afterwards adjusted for by a geometry depending constant, which was determined by relative measurements with the optical power meter (UDT 40X). The focusing lens constant was found using following formula

$$C = I_1 / I_2$$

where C is a focusing exit lens constant; I_1 is the irradiance, measured with an optical spectroradiometer (Optronic 742) with the monochromator set to 450 nm wavelength in 8 nm waveband without focusing exit lens; I_2 is the irradiance, measured with an optical power meter (UDT 40X) with the monochromator set to 450 nm wave-

length in 8 nm waveband with the focusing exit lens.

The absolute energy level for 270, 290 and 310 nm UVR was found by multiplying the focusing exit lens constant (C) with irradiance, measured with spectroradiometer (Optronic 742) for those wavelengths without the focusing exit lens.

Papers II-V

The ultraviolet source was a 150-W xenon high-pressure lamp, mounted in an Oriel 7340 lamphousing (Oriel, Stratford, CT, USA). It was powered by universal power supply (Oriel 68805), stabilized with a light intensity controller (Oriel 68850). The radiation from the source was focused at a monochromator entrance slit by the housing optics. The exit optical beam was focused by a quartz lens, producing a beam size of approximately 4x10 mm^2 at the center of the rabbit cornea (Figure 5). The calibrated Oriel 77250 monochromator was set with a 10 nm waveband at 290 nm (papers II and III) and 310 nm (papers II-V). The energy level in the focus area, used during the rabbit exposures, was measured with a calibrated Laser-Mate/Q detector (Coherent, Auburn, CA, USA).

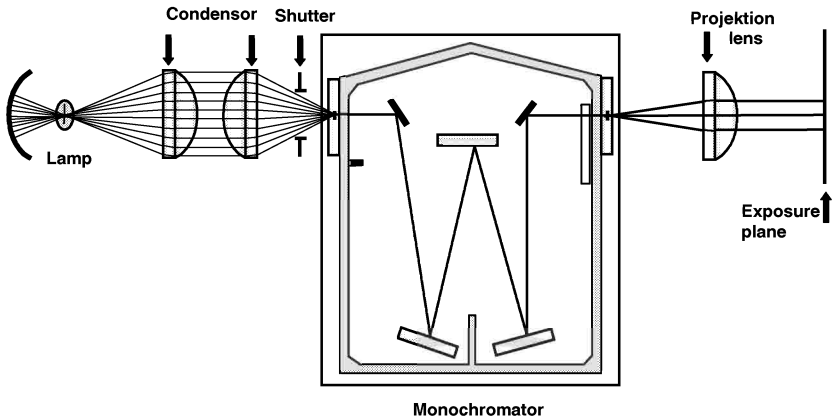

Figure 4. Source of ultraviolet radiation.

2.2 Animals

A total of 79 female adult New Zealand albino rabbits were used, in accordance with the ARVO Resolution on the Use of Animals in Research, and the local ethical committee. Each rabbit received intramuscular Ketalar (ketamine hydrochloride 30 mg/kg) and Rompun (xylazine 5 mg/kg) anesthesia prior to UVR exposure, and a lid speculum was placed. One eye of each rabbit was exposed to UVR.

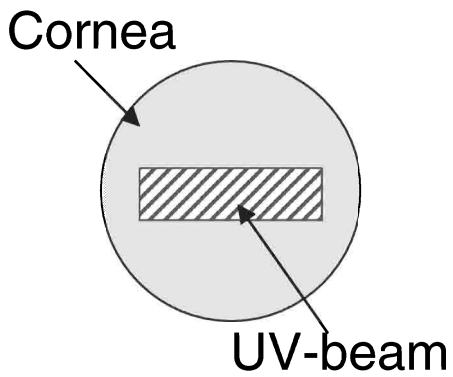

Figure 5. Projection of UVR-beam on the corneal plane.

2.3 Study designs

Paper I

Twenty-four rabbits were used. All rabbits were divided in three groups (Table 1 in I). Group 1 (6 rabbits) was exposed to 270 nm radiant energy. Three of the rabbits were exposed to a subkeratitis dose (0.7 of the corneal threshold dose for keratitis (Hc), or 0.004 J/cm²), and the other three rabbits were exposed to a keratitis dose (3 Hc, or 0.016 J/cm²). Group 2 (6 rabbits) was exposed to 290 nm radiant energy. Three rabbits from this group were exposed to a subkeratitis dose (0.7 Hc , or 0.008 J/cm²), and other three to a keratitis dose (3 Hc, or 0.04 J/cm²). Group three (12 rabbits) was exposed to 310 nm radiant energy in both a subkeratitis dose (3 rabbits; 0.7 Hc, 0.03 J/cm²) and a keratitis dose (9 rabbits; 3 Hc, or 0.14 J/cm²). The corneal threshold doses for different wavelengths has been reported by Pitts et al .[130,160]

The rabbits from group 1 and 2 were sacrificed with an overdose of intravenous pentobarbital three days after exposure. Those rabbits from group 3, exposed to a subkeratitis dose were likewise sacrificed three days after exposure. Three rabbits from group 3 exposed

to a keratitis dose were sacrificed at each time interval: three, seven and fourteen days after exposure. The fellow eye in each rabbit served as a control. The corneas were excised from the exposed and unexposed eyes. The corneas were fixed in four per cent buffered formaldehyde containing one per cent cetylpyridinium chloride. They were then embedded in paraffin.

The sections were double stained with Mayer's hematoxylin and histochemically for hyaluronan.

Paper II

Fourteen rabbits were used. The rabbits were divided in two groups. The first group (7 rabbits) was exposed to 280 nm UVR at a dose producing biomicroscopically significant keratitis (0.12 J/cm^2, or 10 corneal threshold doses for keratitis). The second group (7 rabbits) was exposed to 310 nm UVR likewise at dose producing biomicroscopically significant keratitis (0.47 J/cm^2, or 10 corneal threshold doses).

Four rabbits in each group were sacrificed with an overdose of intravenous pentobarbital 24 hours after exposure. The remaining three rabbits in each group were sacrificed 76 hours after exposure. The fellow eye of each rabbit served as a control. The corneas were excised from the exposed and unexposed eyes. One treated and one untreated cornea from rabbits killed 24 hours after exposure to 280 and 310 nm UVR, respectively, were fixed in 4% glutaraldehyde and prepared for transmission electron microscopy. The remaining corneas were fixed in 4% formaldehyde, embedded in paraffin, and sectioned at 5 µm. The sections were double stained with Mayer's hematoxylin and histochemically for DNA break strands (TUNEL technique).

Paper III

Six rabbits were used. One eye of each rabbit was exposed to UVR. The fellow eye of each rabbit served as a control. The rabbits were

divided in two groups. The first group (3 rabbits) was exposed to 280 nm UVR at a dose producing biomicroscopically significant keratitis (0.12 J/cm^2, or 10 corneal threshold doses for keratitis). The second group (3 rabbits) was exposed to 310 nm UVR likewise at dose producing biomicroscopically significant keratitis (0.47 J/cm^2, or 10 corneal threshold doses).

The rabbits were sacrificed with an overdose of intravenous pentobarbital 24 hours after exposure. The corneas were excised from the exposed and unexposed eyes. Then, the corneas were fixed in 4% formaldehyde, embedded in paraffin, and sectioned at 5 μm. The sections were double stained with Mayer's hematoxylin and immunohistochemically for FasL.

Paper IV

Fifteen rabbits were used. One eye of each rabbit was exposed to UVR at 310 nm at a dose producing biomicroscopically significant keratitis (0.47 J/cm^2, or 10 corneal threshold doses for photokeratitis).

The rabbits were divided in two groups. The first group (9 rabbits) received a single dose of UVR (0.47 J/cm^2 at 310 nm). The second group (6 rabbits) was irradiated 3 times at 7-day intervals (0.47 J/cm^2 at 310 nm). Rabbits from group 1 were sacrificed using intravenous pentobarbital 24 hours, 7 and 14 days after irradiation (three rabbits for each time interval). Rabbits from group 2 were sacrificed 24 hours and 14 days after the last irradiation (likewise three rabbits for each time interval). The fellow eye of each rabbit served as a control. The corneas were excised from the exposed and unexposed eyes. Then the corneas were fixed in 4% formaldehyde, embedded in paraffin, and sectioned at 5 μm. The corneal tissue specimens were processed for histological analysis using specific staining for HA and the TdT-dUTP terminal nick-end labeling (TUNEL) assay, and were then examined with a light microscope.

The TUNEL positive keratocytes and the total keratocyte density were counted in one 30x high power field per histologic section of the corneas from irradiated eyes 24 hours after UVR exposure in rabbits from group 1 and 24 hours after last UVR exposure in rabbits from group 2. The microscope field during cell counting was placed in the center of the UVR exposed area comprehending the whole thickness of the corneal section.

The HA staining intensity in the corneal stroma during evaluation with a light microscope was graded in the following manner: - no staining; + very weak staining; ++ intense staining; +++ very intense staining.

Paper V

Twenty rabbits were used. Five rabbits were used as a control group, and did not receive any UVR treatment. The remaining 15 rabbits received intramuscular Ketalar (ketamine hydrochloride 30 mg/kg) and Rompun (xylazine 5 mg/kg) anesthesia prior to UVR exposure. One eye of each rabbit was exposed to UVR at 310 nm at a dose producing biomicroscopically significant keratitis (0.47 J/cm^2, or 10 corneal threshold doses). The fellow eye of each rabbit was not exposed to UVR, and served as a second control group.

The UVR exposed rabbits were divided in three groups. The first group (5 rabbits) was sacrificed with an overdose of intravenous pentobarbital 3 days after UVR exposure. The second group (5 rabbits) was sacrificed 7 days, and the third group (5 rabbits) was sacrificed 28 days after UVR exposure. The corneas were excised without the scleral rims from the exposed and unexposed eyes, and immediately processed for the RNA extraction.

2.4 Histochemistry

HA staining (papers I and IV)

The HA-binding region (HABR) of cartilage proteoglycans used in the staining technique was prepared by

affinity chromatography on HA sepharose, as described previously.[161] The purified protein then was linked to biotin according to the principles outlined by Rippelino et al.[162] HA was used during the biotinylation to protect the HA binding site on the HABR and then removed. HABR-protein used in the present study was generously donated by Pharmacia & Upjohn AB (Uppsala, Sweden). After incubation with HABR-biotin for two hours at room temperature, the corneal tissue sections were rinsed in phosphate-buffered saline and incubated for one hour with avidin-biotin-complex Vectastain reagent (Vector Laboratories Inc., Burlingham, CA). The sections labelled with peroxidase were visualised with ethyl carbozole. Control sections were incubated for two hours in a humidified chamber at 37 °C with 50 U/ml of Streptomyces hyaluronidase (Seikagaku Fine Biochemicals, Tokyo, Japan). The sections were counterstained in Mayer's hematoxylin and mounted under coverglass slips in Kaiser's glycerin-gelatin.

The sections were examined in the light microscope.

DNA fragmentation assay (TUNEL) (papers II and IV)

Biochemically, apoptosis can be recognized by extensive cleavage of cellular DNA into oligonucleosome-sized fragments. For this reason, apoptosis was evaluated using the commercially available ApopTag modification (Oncor, Gathersburg, MD, USA) of the terminal deoxynucleotidyl transferases (TdT)-mediated dUTP-digoxigenin nick end labeling (TUNEL) technique.[163] Paraffin-embedded, 5 μm sections were deparaffinized and rehydrated through graded alcohols. Protein was digested by treating the tissue slides with pronase at 37°C for 5 minutes, after which endogenous peroxidase was quenched by 2% hydrogen peroxide for 5 minutes. The ApopTag processing then included the application of two drops of an equilibration buffer directly to each

specimen, followed by 10-15 seconds incubation beneath a plastic coverslip. After removal of the coverslip, 54 µl of working strength deoxynucleotidyl transferase was applied directly to each specimen. The slides were then incubated for 1 hour beneath a plastic coverslip in a humidified chamber at 37°C. Following removal of the plastic coverslip, each specimen was put in a coplin jar containing pre-warmed working strength stop/wash buffer and incubated for 30 minutes at 37°C. Two drops of anti-digoxigenin peroxidase were then applied to each specimen. These were then incubated in a humidified chamber for 30 minutes at room temperature. Finally, sections were stained with 3-amino-9-ethylcarbazole, counterstained with hematoxylin, and mounted.

Positive controls were obtained from the manufacturer, using formaldehyde-fixed, paraffin embedded sections from female rodent mammary gland, retrieved 3-5 days after weaning of rat pups. Some specimens from UV-exposed corneas were used as negative controls by substituting 32 µl of distilled water for deoxynucleotidyl transferase from the protocol, as suggested by manufacturer and others.[164-166]

The sections were then examined in the light microscope.

Fas ligand staining (paper III)

Binding of Fas ligand to Fas receptor leads to induction of intracellular signals that eventually result in apoptotic cell death. To study the expression of Fas ligand protein in the rabbit cornea, immunohistochemistry was performed using standard methods involving biotinylated secondary antibodies and streptavidin-conjugated peroxidase according to the manufacturer's instructions (SantaCruz ™ Staining System, cat # sc-2053; Santa Cruz Biotechnology, Santa Cruz, CA, USA). A polyclonal anti-FasL goat antibody (FasL N-20; Santa Cruz Biotechnology) was used as primary antibody at a concentration 2 µg/ml. Some specimens from unexposed

and UVR exposed corneas were used as negative controls by preincubating the antibody with sc-834P control FasL peptide (Santa Cruz Biotechnology) at a concentration of 20 µg/ml for 30 minutes before incubating with tissue sections. The sections were counterstained in Mayer's hematoxylin and mounted under coverglass slips in Kaiser's glycerin-gelatin.

The sections were examined in the light microscope.

2.5 Transmission electron microscopy (TEM) (paper II)

Corneas for transmission electron microscopy were fixed in 4% glutaraldehyde, osmicated, and stained with uranyl acetate. They were then serially dehydrated, embedded in Epon, sectioned at 60 nm, and placed on formvar-carbon coated copper grids. The examination was performed with a JEM 1200-EX electron microscope (JEOL, Tokyo, Japan).

2.6 Reverse transcriptase polymerase chain reaction (RT-PCR) for biglycan (paper V)

Reverse transcriptase polymerase chain reaction was used to study the expression of biglycan gene in the rabbit cornea.

RNA extraction

The corneas were suspended in 1 ml of ice cold RNAzol B (Biotecx Laboratories, Houston, TX, USA), and the total RNA was extracted according to the manufacturer's instructions. The final RNA pellets were resuspended in 40 µl diethylpyrocarbonate-treated water containing 1 U of RNAsin (Life Technologies, Täby, Sweden), and DNase I treated (Promega, Madison, WI, USA), followed by phenol/chloroform extraction and ethanol precipitation of the samples. The integrity of the RNA samples was analyzed on an 1% agarose gel (Life Technologies) containing ethidium bromide (0.5 µg/ml). RNA was stored at -80°C until further analysis. All samples were normalised to

contain equal amounts of the total RNA. RNA concentration was measured using spectrophotometer, and 150 ng of RNA were used in reverse transcription reaction. This procedure compensated for unequal size of the samples and differences in RNA extraction. First strand cDNA synthesis of total RNA was performed by using M-MLV reverse transcriptase (Life Technologies), and hexamer primers, $pd(T)_6$ (Pharmacia Biotech, Uppsala, Sweden).

Construction of internal standards

Primers for biglycan were used according Hellio le Graverand et al (Table 1 in V).[167] PCR amplification of a 406 bp long biglycan cDNA fragment was performed in a total volume of 25 μl, containing 1 μl of cDNA, using an iCycler Thermal Cycler (BioRad, Hercules, CA, USA). The other reaction constituents included 0.75 mM $MgCl_2$, 10 mM Tris HCl, 50 mM KCl (all from Life Technologies), 0.2 mM dNTPs (Pharmacia), 0.1 mM of each biglycan primer (Table 1) and 0.5 U of Taq polymerase (Life Technologies). The reaction was conducted for 35 cycles under the following temperature conditions: denaturation at 95°C for 30 sec, annealing at 60°C for 30 sec and elongation at 72°C for 30 sec, followed by a final extension step at 72°C for 5 min. The PCR products were separated on a 1.5% agarose gel and purified.

The biglycan internal standard was constructed by the introduction of a deletion in the biglycan gene.[167] The forward primer generating the deletion in amplification fragment was designed (Table 1 in V). The 272 bp long final biglycan internal standard was created by a PCR amplification of the biglycan fragment and purification from an agarose gel. The concentration of the internal biglycan standard thus obtained was determined by comparison with known amounts of Low DNA Mass™ Ladder (Life Technologies).

Another set of primers produced a 293 bp-long glyceral-

dehydes 3-phosphate dehydrogenase (GAPDH) gene fragment (Table 1 in V).[168] Amplification of this fragment generating the deletion was performed as described for the biglycan internal standard. After amplification and purification from an agarose gel, a 190 bp long internal GAPDH standard was obtained.

Competitive RT-PCR

Competitive PCR was performed in a total volume of 25 µl, including 2 µl of cDNA (in appropriate dilutions determined in preliminary PCR experiments) as well as 1 µl of each internal standard in 5 different concentrations: 10^{-5}-10^{-3} attomoles/µl for both GAPDH and biglycan.

The PCR products were separated on a 2% agarose gel. The ethidium bromide stained gel was photographed under UV-light with the DC120 Digital Zoom Camera (Eastman Kodak Company, Rochester, NY, USA). The molar ratio between the concentrations of the biglycan gene PCR product and the house-keeping gene GAPDH gene product was calculated for each specimen after determining the intensity of the ethidium-bromide-stained bands visually.

Validation of the competitive RT-PCR method

The exponential amplification range of the RT-PCR was determined by performing the reactions with different numbers of cycles (20-50 cycles) in order to avoid the so-called "plateau" effect.

The purity of each RNA preparation was verified, since the presence of DNA contamination causes false positive reactions or overestimation of the transcripts obtained. To monitor this, we selected controls for each set of assays: 1) a positive control (rabbit cartilage cDNA), 2) a sample in which the reverse transcription step had been omitted to detect contaminating genomic DNA, and 3) reagent controls containing all the necessary components for PCR, but no template.

2.7 Statistical analysis (paper V)

Since the observations were not normally distributed, Kruskal-Wallis one way analysis of variance was used for testing the differences between the groups. Thereafter, nonparametric multiple comparisons were performed in order to locate the differences among the groups. The probability (p) level of <0.05 was considered significant.

3. RESULTS

3.1 Cellular response and production of hyaluronan (paper I)

None of the control corneas showed any cellular damage or epithelial or stromal HA staining.

Corneas exposed to UVR at 270, 290 and 310 nm at sub-keratitis doses showed no morphological changes or staining of HA in corneal epithelial or stromal cells.

Corneas exposed to 270 and 290 nm UVR at keratitis doses showed a relative loss of epithelial cell layers three days after exposure. Approximately two to three epithelial cell layers were present at that time. No changes were detected in the keratocytes, nor was any abnormal HA production detected.

Corneas exposed to 310 nm UVR at keratitis doses showed at day three a thin, not completely repaired epithelium (two-three cell layers) (Figures 1A and 1B in I). The corneal stroma was seriously damaged in the central part. Keratocytes had disappeared completely throughout the entire stromal thickness of the central cornea. Only keratocyte fragments were left. This damaged area was surrounded by a front of keratocytes. The staining for HA was found in the immediate vicinity of the keratocytes at the border of the damaged area. Hyaluronan was all the time strictly associated with the keratocytes. The peripheral parts of the cornea were unaffected.

By seven days, the epithelium had healed in corneas exposed to 310 nm UVR. Much of the damaged area had now been populated by keratocytes. These cells all stained positive for HA. However, the anterior one fourth of the corneal stroma was still free of keratocytes in the injured zone (Figures 2A and 2B in I). Still, staining for HA was strictly confined to the keratocytes.

At fourteen days, all specimens showed a completely repaired stroma repopulated by keratocytes. Only a faint red stain for HA could be traced in the posterior stroma surrounding some kerato-

cytes, near Descemet's membrane (Figures 3A and 3B in I).

3.2 Apoptosis after single exposure (paper II)

DNA fragmentation assay (TUNEL)

None of the unexposed corneas, stained with TUNEL technique, showed any positive signals in the keratocytes or endothelial cells (Figure 1A in II). Positive TUNEL staining in the unexposed corneas was limited to a few superficial epithelial cells. No positive staining was detected in any of the negative controls. In contrast, all corneas, exposed to UV-radiation, showed drastically increased number of positive stained cells in the treated area.

Evaluation of corneas, exposed to 280 nm UVR, showed at 24 hours loss of epithelial cells. Only one or two epithelial cell layers were present. There was a large number of epithelial cells and superficial keratocytes that were stained TUNEL-positive (Figure 1B in II). The remaining stroma and the endothelial layer were unaffected. Seventy-six hours after exposure the epithelium consisted of two or three cell layers with only a few TUNEL-positive epithelial cells. The stroma and the endothelial layer were normal.

Corneas, exposed to 310 nm UVR, showed at 24 hours likewise loss of epithelial cells with two or three layers left. TUNEL assay showed extensive positive signals in the epithelial cells, in almost all keratocytes in the entire thickness of the corneal stroma in the treated area, and also in endothelial cells (Figure 1C and 1D in II). The peripheral parts of the corneas were unaffected. Seventy-six hours after exposure keratocytes disappeared completely in the entire thickness of the central stroma. Only keratocyte fragments remained (Figure 1E in II). The positive TUNEL staining was limited to a few epithelial cells at that time point.

No signs of inflammation, such as presence of leukocytes or monocytes, were found in

any corneas, 24 and 76 hours after exposure.

Transmission electron microscopy

Transmission electron microscopy evaluation of corneas from each group confirmed the results received using the TUNEL assay. None of the corneas from unexposed eyes had any cellular damage. No apoptotic cells were detected in those corneas. Twenty-four hours after exposure to 280 nm UVR epithelial cells and keratocytes immediately beneath the epithelial basement membrane, had signs consistent with apoptosis: cell shrinkage, condensation and fragmentation of chromatin, and cellular blebbing with the formation of membrane-bound structures that appeared to be apoptotic bodies (Figure 2A in II). Phagocytes also were identified in the affected area.

In corneas, exposed to 310 nm UVR and analyzed 24 hours after exposure, signs of apoptosis were found even in keratocytes in the deep stroma and in the endothelial cells (Figures 2B and 2C in II).

3.3 Expression of Fas ligand protein (paper III)

None of the negative controls showed any positive FasL staining. FasL protein was uniformly detected in epithelial and endothelial cells in both UVR exposed and unexposed corneas (Figures 1A and 2A in III). The positive staining was always associated with cell membranes, and it was evenly distributed through the entire epithelial and endothelial cell layers. There was no difference in staining pattern of epithelial and endothelial cells between UVR exposed and unexposed corneas.

No positive staining was detected in the keratocytes in the unexposed corneas (Figure 1A in III). All corneas, exposed to 280 nm UVR, showed positive FasL staining of keratocytes in the anterior one fourth of the corneal stroma in the UVR treated area (Figures 1B and 2B in III). There was even a few posterior keratocytes that were stai-

ning positively for FasL in this group. The positive keratocyte staining in the all corneas, exposed to 310 nm UVR was much more intensive and extended throughout the entire thickness of the stroma in the UVR treated area (Figures 1C and 2C in III). The FasL staining was associated with the cell membranes. No positive staining keratocytes were found outside the treated area.

3.4 Comparison of apoptosis after single and repeated exposures (paper IV)

DNA fragmentation assay (TUNEL)

None of the unexposed corneas, stained with TUNEL technique, showed any positive signals in the keratocytes or endothelial cells. Positive TUNEL staining in the unexposed corneas was limited to a few superficial epithelial cells. No positive staining was detected in any of the negative controls. In contrast, UVR-exposed corneas showed increased number of positive staining cells in the treated area.

All corneas exposed to a single dose of UVR, showed at 24 hours extensive positive signals in epithelial cells. So did almost all keratocytes in the entire thickness of the corneal stroma in the treated area, and also some endothelial cells (Figure 1A and Table 1 in IV). The peripheral, unexposed parts of the corneas were unaffected. At day 7 and 14 no positive signals in the stroma or the endothelium were detected. In the epithelium positive staining was found in a few superficial cells as in the fellow unexposed cornea.

All corneas, exposed to repeated doses of UVR, showed 24 hours after the last exposure positive TUNEL staining in epithelial cells. The staining was as extensive in distribution and intensity as after a single exposure. A completely different staining pattern was detected in the stroma and the endothelium. Positive staining was found only in very few stromal cells (Figure 1B

and Table 1 in IV), and no positive staining was detected in the endothelium. At day 14 after the last exposure no positive staining in the stroma or endothelium was found, and the staining pattern of the epithelium was the same as that of the fellow cornea.

The cell counting 24 hours after UVR exposure showed a lower total number of keratocytes in the corneas that received repeated UVR doses compared to the corneas that received a single UVR dose. However, the percentage of TUNEL positive keratocytes was considerably higher in corneas received a single UVR dose (Table 1 in IV). The differences between these two groups were considerable, but the limited number of animals prevented significance.

3.5 Expression of hyaluronan after single and repeated exposures (paper IV)

None of the unexposed corneas showed any cellular damage or epithelial or stromal HA staining. Likewise no positive staining was found in the specimens that served as negative controls.

All corneas exposed to a single dose of UVR, showed at 24 hours relative loss of epithelial cells with two-three layers left. No positive staining for HA was found in the epithelium or stroma. Extracellular HA staining of high intensity was found at day 7 (Figure 2A and Table 2 in IV). This staining was present throughout the entire central stroma, except the anterior one-fourth immediately underlying the epithelium. HA was always strictly associated with keratocytes. At day 14 only a faint HA staining was detected in the posterior stroma, close to the Descemet‘s membrane (Figure 2B and Table 2 in IV).

All corneas, exposed to repeated UVR, showed positive staining of very high intensity both at 24 hours and at day 14 after the last UVR exposure (Figures 2C, 2D and Table 2 in IV). HA was evenly distributed throughout the entire thickness of the corneal stroma. HA

deposits were often unassociated with keratocytes. From evaluation in the light microscope, the HA staining was equally intense at 24 hours and day 14 in corneas exposed to repeated UVR.

3.6 Levels of biglycan gene expression (paper V)

The results of the competitive reverse transcription polymerase chain reaction are shown in Table 2 (in V). The competitive RT-PCR was performed twice with each specimen, and the results were repeatable. GAPDH mRNA expression was observed in all specimens. There was no expression of biglycan mRNA in the control group consisting of corneas from normal unexposed rabbits. Three days after exposure to UVR biglycan mRNA was still not expressed. Seven days after exposure biglycan mRNA was markedly expressed in the UVR treated corneas ($p<0.05$). The expression of biglycan mRNA had decreased at 28 days after exposure in the UVR treated corneas, however, there was no significant difference compared with the other three groups.

4. DISCUSSION

4.1 Action of different UVR wavelengths and doses on the cornea

The degree of damage produced by UVR depends on several factors such as applied wavelengths and exposure time.[169,170] Wavelengths below 290 nm are almost completely absorbed by the epithelium and do not penetrate the deeper lying eye structures.[131,171] In contrast, the middle (300-320 nm) wavelengths are known to be absorbed by corneal stroma and lens.[131,171] Previous ultrastructural studies have shown that the corneal stroma exposed in the 290 nm wavelength range and shorter was resistant to UVR damage, even if the exposures was as high as 100 times the threshold level to produce photokeratitis.[170] At the same time exposures in the 300 nm range and longer cause stromal oedema, keratocyte damage and stromal opacification.[130,172-175]

Our experiment, at the microscopic level, showed a similar pattern: exposure to UVR in range ≤290nm in photokeratitis doses resulted in the superficial corneal damage. Twenty-four hours after UVR exposure, apoptosis was found in the epithelium and in the superficial keratocytes only. At the same time corneas exposed to 310 nm UVR in photokeratitis doses showed a deep damage through all corneal layers. Twenty-four hours after UVR exposure, apoptotic cells were found in the epithelium, the keratocytes through the entire thickness of the stroma, and in the endothelial cells. The extent of the keratocyte free area in the stroma 3 days after UVR exposure was large and evident, from the superficial stroma throughout to the Descemet's membrane.

No epithelial or stromal damage was found following a subkeratitis exposure after three days, nor any endothelial damage.

4.2 Mechanisms of the corneal cellular damage after UVR exposure

Programmed cell death, or apoptosis, is a fundamental process that plays a critical role during tissue development, homeostasis, infection, wound healing, and pathophysiology of disease in many organs.[178-180] In contrast to necrosis, apoptosis is a form of involutional cell death with limited inflammation and without release of cellular contents that would inflict collateral damage to surrounding tissue.[180-182] Apoptosis is recognized morphologically by cell shrinkage, condensation of chromatin into dense masses attached to the nuclear membrane, formation of apoptotic bodies, and phagocytosis.[181,183] Biochemically, apoptosis can be recognized by extensive cleavage of cellular DNA into oligonucleosome-sized fragments.[184,185] Although apoptosis is not found normally in the corneal stroma and endothelial layer, limited number of apoptotic cells can be identified in the superficial epithelium.[186]

Apoptosis within the corneal epithelium has been inferred from the discovery of the dark cells during the regeneration stage in the rat corneal epithelium after chemical abrasion.[187] It has been suggested that similar dark cells could represent deletion within the epidermis because of hyperproliferation.[188.189] However, dark cells have also been described in the corneal epithelium as result of the damage caused by UV-radiation.[190] Using transmission electron microscopy, Ringvold et al[172] found keratocytes with nuclear fragments of high electron density and abnormal inclusions in the rabbit corneal stroma after UVR exposure.

The present study, based on a combination of *in situ* nick end labeling and electron microscopy, clearly defined that apoptosis is one important mechanism of corneal cell death after UVR exposure at photokeratitis doses. TUNEL assay showed obvious differences between normal and irradiated corneas.

Transmission electron microscopy evaluation of corneas confirmed that cells in locations where staining occurred in the TUNEL assay had morphologic changes, including cell shrinkage, chromatin condensation and fragmentation, and cellular blebbing, consistent with apoptosis. The lack of leukocyte infiltration confirms the absence of a necrotic process.

Although our impression was that the epithelial injury produced from 280 nm UVR was deeper than that produced from 310 nm, the stromal damage appeared to be minimal in those corneas. However, different types of epithelial injury, such as manual deepithelialization, scalpel or microtome incisions, herpes simplex virus infection, and excimer laser surgery, may trigger apoptotic cell death of deeper lying keratocytes through release of cytokines (IL-1).[191-194] Our results indicate that this mechanism of keratocyte apoptosis can be implicated only in case of shorter UVR wavelengths. The fact that it was much deeper stromal damage in corneas that were exposed to 310 nm UVR leads to a conclusion that UVR at 310 nm may activate keratocyte apoptosis directly, without involvement of cytokines released from injured epithelium.

At the present time known molecular mechanisms that have capacity to trigger apoptosis in keratocytes include IL-1 receptor and Fas receptor activation.[177,195] Fas receptor is expressed in epithelial, keratocyte, and endothelial cells in normal unwounded human cornea.[195] Fas ligand (FasL) is expressed in epithelial and endothelial cells, but not in the keratocytes in the unwounded human cornea.[195,196] Binding of FasL to Fas receptor leads to induction of intracellular signals that eventually result in apoptotic cell death.[197-199] Both Fas and FasL were initially characterized as membrane-bound proteins, suggesting that direct cell to cell interaction is necessary for activation of Fas system.[200-202] Recent studies have demonstrated

that Fas and FasL are also expressed as soluble cytokines.[203-205] Soluble Fas, similar to numerous other soluble cytokines and growth factor receptors, has been shown to compete with membrane-bound Fas for available FasL preventing apoptosis in the normal epithelial and endothelial cells which constitutively express both Fas and FasL.[206-209] It has been described by Mohan et al[205] that IL-1 release from corneal epithelium after injury may induce FasL expression in keratocytes and trigger keratocyte apoptosis through autocrine mechanisms since the keratocytes constitutively express Fas receptor.

In the current study, we found that the FasL expression in the keratocytes was very similar in distribution to that of apoptosis after UVR exposure. Positive FasL staining in the keratocytes was confined to the anterior stroma in the corneas that were exposed to 280 nm UVR. The expression of FasL in the keratocytes in those corneas that were exposed to 310 nm UVR was much more widespread and extended throughout the entire thickness of the stroma in the treated area. The pattern of FasL expression in the stroma of the UVR exposed corneas and the fact that FasL was not found in the stroma in the unexposed corneas strongly suggests that FasL is involved in the regulation of apoptosis in the corneal cells after UVR exposure. Also, we confirmed in the current study the previously described finding that FasL is expressed in the epithelial and endothelial cells in normal unwounded corneas.[195,196]

The explanation of why 310 nm UVR produces more extensive FasL expression and subsequent apoptosis in the corneal stroma than 280 nm, can be based on a different absorption pattern of these wavelengths in the cornea. Thus, it is known that UVR in 280 nm range is almost completely absorbed by the epithelium, while 310 nm UVR is known to be absorbed also in corneal stroma. The pattern of FasL expression and

apoptosis in the corneal stroma indicate that UVR at 310 nm may activate directly the Fas/FasL system in keratocytes, independent from the release of IL-1 from injured epithelial cells. This hypothesis is supported by the fact that both 280 and 310 nm UVR gave equally deep epithelial damage, while stromal damage was much bigger after exposure to 310 nm UVR.

4.3 Role of hyaluronan in the corneal repair after UVR exposure

The hydration, thickness and transparency of the mammalian cornea is thought to be related to the stromal glycosaminoglycan and proteoglycan content. Hyaluronan (HA) is classified among the glycosaminoglycans (GAG), and is a repeating disaccharide composed of glucuronic acid and N-acetylglucosamine. HA is characterised by its unique capacity to immobilize large amounts of water and ions, and affect extracellular compartmentalization of macromolecules.[210-214] Although HA is not normally found in the corneal stroma, several investigators have described that HA is produced in cultures of rabbit and human stromal cells.[215-220] HA binding sites and trace amounts of HA have been identified on the apical surface of the corneal endothelium in normal corneas.[44,46,221]

We found, in the present study, that extensive apoptosis occurring after UVR exposure at a photokeratitis dose at 310 nm triggered reactive formation of HA. Other investigators have shown that apoptotis initiating cytokines, such as IL-1 and soluble Fas, can stimulate HA production in fibroblast cultures.[222,223] Yet, other cytokines participating in the corneal wound healing, such as transforming growth factor beta (TGF-β) and platelet-derived growth factor (PDGF), upregulate expression of hyaluronan synthase, the enzym protein involved in HA biosynthesis, by cultured corneal endothelial cells.[224]

Positive HA staining was strictly confined to the kerato-

cytes all the time. It was the keratocytes that was on the border of the cell free area that stained positive for HA. We believe that this can be a sign of a cell preparedness to move and repopulate the damaged stroma. Several investigators have described the HA production in the chick embryo during a period of corneal stromal swelling and invasion by mesenchymal cells. Later, the action of hyaluronidase in the stroma leads to decreased levels of HA, stromal dehydration, and corneal transparency.[225-227] HA may create hydrated spaces for cell movement and also form a coat around migrating cells that would block or weaken adhesion to other cells, preventing immobilization or precocious development.[225] Yet, other investigators found that HA stimulates migration of corneal epithelium, and that HA plays an important role in cell proliferation, and differentiation.[227-231] Longaker et al[232] reported a prolonged presence of HA in the matrix of fetal wounds. The presence of HA creates a "permissive" wound environment that promotes fetal fibroblast movement and proliferation, and inhibits cyto-differentiation that allows healing by regression without fibrosis or scar formation. The production of HA in the healing cornea therefore may represent a capacity for the keratocyte to regress to an earlier stage of development during healing. HA was surrounding the keratocytes only during the repopulation phase of the wound healing. When the keratocytes had repopulated the stroma at 14 days after acute UVR exposure, HA disappeared.

4.4 Action of single and repeated UVR doses on the cornea

Chronic exposure to UVR has been associated with an increased risk of several corneal disorders, including pterygium, climatic droplet keratopathy, and climatic proteoglycan stromal keratopathy.

It was shown in the present study that a single exposure to UVR leads to production of HA.

The maximum expression of HA was present at day 7 after UVR exposure, and 14 days after UVR exposure HA had disappeared almost completely. In contrast, corneas exposed to repeated doses of UVR, showed very intense positive staining for HA also 14 days after the last exposure. This suggests that repeated UVR exposures lead to an increased production and accumulation of HA. Such a production and accumulation of HA may be a sign of long-term changes in the cornea that can lead to corneal haziness and, eventually, to development of corneal degeneration. Haze development after excimer laser surgery and surgical wounds has been associated with deposition of HA in the corneal stroma.[47-50]

An alternative possibility is that repeated UVR could damage some at this time unknown mechanisms of HA degradation in the cornea. It has been described earlier that HA from the aqueous in the rabbit eye is catabolized in the liver.[233] The turnover mechanisms of HA in the cornea are still not completely clarified. Recently, it has been reported that the membrane bound HA receptor (CD44) mediates a transportation of extracellular HA into the cytoplasm of transformed fibroblasts and alveolar macrophages, where HA can be destroyed by lysosomes.[234] CD44 is normally expressed on basal epithelial cells, keratocytes and endothelial cells in rabbit cornea.[235] Hyaluronidase, an endoglycosidase that degrades HA and other glycosaminoglycans, has been demonstrated immunohistochemically in endothelial cells in sections from normal adult human cornea.[236] Further investigations into whether CD44 or hyaluronidase could be damaged by UVR are needed.

The total number of keratocytes was lower 24 hours after the last exposure in the corneas that received repeated UVR doses compared to a single dose. The possible explanation to this fact could be a non-complete keratocyte repopulation of the damaged central

stroma after the first two UVR exposures. However, the fraction of apoptotic cells among stromal and endothelial cells (percentage of TUNEL positive cells) was also considerably lower in the corneas after repeated UVR exposures, suggesting an increased resistance to apoptosis of those cells. The increased HA production, and the resistance to apoptosis could be due to a change in phenotype of the corneal cells. Recently, it has been reported that repeated epithelial scrapings reduce the level of apoptosis of keratocytes in the underlying anterior stroma.[237] One could also hypothesize, that the presence of HA after repeated UVR exposures may be one of possible mechanisms protecting the corneal cells against further damage. Thus, it has been suggested earlier that the presence of HA in the anterior chamber of the eye could be a system for scavenging of free radicals.[238,239] Furthermore, it has been reported that hydroxyl radical formation after excimer laser photoablation is an important mechanism leading to keratocyte apoptosis.[240]

It has been suggested earlier that metallothionein (MT), a protein that is involved in metal detoxification, homeostasis, and scavenging of free radicals during oxidative damage, is synthesized by different cell types after exposure to ionizing radiation or UVR.[241-243] The synthesis of MT is considered as one of the mechanisms involved in the adaptive response to low dose radiation exposure. It remains to be clarified whether this mechanism is involved in the adoption of corneal cells to repeated UVR exposures.

4.5 Biglycan a novel marker of corneal wound healing

Biglycan is a dermatan sulfate proteoglycan. Recently, Funderburgh et al[55] found very small amounts of biglycan protein in the normal human corneal epithelium and stroma using immunoblotting. Stromal biglycan deposits have been identified in corneas with keratoconus, bullous keratopathy, edema,

and scars.[55,56] In the present study we have used the sensitive molecular technique of competitive reverse transcription polymerase chain reaction to analyze RNA isolated from the corneas of rabbits exposed to UVR and non-exposed control corneas to assess transcripts for biglycan. Our data show that the biglycan gene is not expressed in the normal rabbit corneas. Similarly, Bianco et al[54] have described using in situ hybridization, that biglycan gene is not normally expressed in the human cornea. Significant biglycan mRNA expression was noted at 7 days after UVR exposure. At that time point the corneas revealed a stromal edema and slight haze during examination by slit lamp. The expression of biglycan mRNA had decreased at 28 days after UVR exposure, and the corneas appeared normal in the slit lamp. This pattern of biglycan gene expression strongly suggests that biglycan is involved in the process of corneal wound healing after UVR exposure at photokeratitis doses.

The role of biglycan in corneal wound healing is a matter of speculation. It has been described that biglycan is expressed in tissues with an active morphogenesis and differentiation, suggesting that biglycan is involved in the regulation of these processes.[54] Treatment of cultured keratocytes by transforming growth factor beta (TGFβ) leads to marked expression of biglycan during transdifferentiation of keratocytes to the myofibroblastic phenotype.[244]

The peak of biglycan production was seen, similarly to HA, at 7 days after UVR exposure. One could speculate that biglycan co-operates with hyaluronan during corneal wound healing. Thus, it has been described that biglycan is able to associate with hyaluronan.[245] Biglycan may create a network that holds hyaluronan in the corneal stroma, preventing an early disappearance of hyaluronan from the stroma, and allowing the complete repopulation of the stroma by keratocytes after UVR damage. One

of the properties of the endogenously produced hyaluronan is to serve as a provisional matrix during repair after severe corneal injuries.[48] Why hyaluronan has these unique properties may be in part explained by interaction with biglycan.

5. GENERAL CONCLUSIONS

- A photokeratitis dose of 310 nm UVR is needed to cause significant keratocyte damage. A photokeratitis dose of shorter wavelengths causes damage to epithelial cells and superficial keratocytes only, due to a very high absorption of these wavelengths in the epithelium.
- Apoptosis, initiated by Fas/Fas ligand system activation, is one important mechanism leading to the corneal cell death after UVR exposure.
- A photokeratitis dose of 310 nm UVR initiates apoptosis through the entire corneal thickness.
- The keratocyte production of HA appears to be a sign of cell readiness to repopulate the damaged stroma devoid of keratocytes after UVR exposure.
- Repeated UVR exposures lead to increased production and accumulation of HA in the corneal stroma. The repopulated keratocytes are much more resistant to apoptosis than the native ones. HA accumulation is another sign of long term changes that may lead to development of corneal degeneration.
- There is no expression of biglycan gene in the normal rabbit cornea. UVR exposure leads to a distinct expression of biglycan gene in the rabbit cornea that decreases 4 weeks after exposure indicating the biglycan involvement in the corneal repair process. Biglycan appears to be a novel marker of the corneal wound healing.

6. ACKNOWLEDGEMENTS

Many people have supported me during my PhD training. I would like to specially thank the following persons, institutions and foundations:

- Professor Per Fagerholm, my tutor and mentor, for inviting me to the world of science, for his unfailing support and friendship.
- Professor emeritus Bo Lindström, for his help in the critical evaluation of the data and his masterful teaching of medical statistics.
- Professor Gunnar Lennerstrand, for his kind support during my PhD thesis work.
- Professor emeritus Björn Tengroth, for his comments and for his achievement to create excellent research and clinical facilities at St Erik's Eye Hospital.
- Assoc. Professors Magnus Gjötterberg and Stefan Seregard, and Drs Sven-Olov Ingemansson and Sven Blomdahl, for their kind help during my clinical work at St Erik's Eye Hospital and Huddinge University Hospital.
- Assoc. Professor Ingeborg van der Ploeg, for inviting me to the world of molecular biology and for constructive criticism of my work.
- Drs Louise Bergman and Peder Jahnberg, for their friendship and for teaching me retinal surgery.
- Drs Santiago Tomas Barberan, Lisha Gan, Beat Weber, Manoj Kakar, Vino Mody, Xiuqin Dong and all research colleagues and staff at St Erik's Eye Hospital for friendship and all interesting discussions about cultural differences.
- Marina Koulikovska, my co-author, for helping me in research and being my friend.

- Lab technicians Margareta Oscarsson, Berit Spångberg, Anne Winter-Vernersson, Agneta Bonnevier, and Ylva Lagerqvist, for their skilful assistance in histology and computer graphics.
- Photographer Maud Leindahl, for friendly help with film developing and copying.
- Secretaries Britt-Marie Karlheden, Ulla-Britt Schützler-Peterson, and Claire Johansson, for nice help with all bureaucratic work.
- Animal care technician Monica Aronsson for keeping the animals in good mood and condition.
- My family and all my friends. Without your love and support this work would never had been done!

Generous financial support was received from:

- Karolinska Institutets resebidragsstiftelser
- Hildur Petterssons stiftelse
- Kronprinsessan Margaretas arbetsnämnd för synskadade
- Synfrämjandets forskningsfond
- Margit Thyselius fond
- Universitetssjukhusets i Linköping fond för medicinsk forskning
- Swedish Medical Research Council
- Karin Sandquists stiftelse

7. REFERENCES

1. O'Rahilly R. The prenatal development of the human eye. *Exp Eye Res*. 1975;21:93-112.
2. Ewer MS. Early development of the stroma corneae and the pupillary membrane in man. *Acta Anat (Basel)*. 1970;75:37-46.
3. Marshall J, Grindle CF. Fine structure of the cornea and its development. *Trans Ophthalmol Soc U K*. 1978;98:320-8.
4. Nishida T. Basic Science: Cornea, sclera, and ocular adnexa. Anatomy, biochemistry, physiology, and biomechanics. In: J.H. Krachmer (Ed.), *Cornea* (Vol. Fundamentals of Cornea and External Disease, pp. 3-198). St. Louis: Mosby.
5. Schwarz W, Keyserlingk DG. On the fine structure of the human cornea with special reference to the problem of transparency. *Z Zellforsch Mikrosk Anat*. 1966;73:540-8.
6. Thiel HJ. Epithelium of the cornea and its significance for transparency. *Dtsch Med Wochenschr*. 1974;99:1630-5.
7. Dupoisot HF. The corneal stroma and its physical properties. *C R Seances Acad Sci D*. 1979;288:239-41.
8. Seiler T. Transparency of the cornea. *Fortschr Ophthalmol*. 1987;84:115-7.
9. Axelsson I. Heterogeneity, polydispersity, and physiologic role of corneal proteoglycans. *Acta Ophthalmol (Copenh)*. 1984;62:25-38.
10. Conrad GW, Funderburgh JL. Eye development and the appearance and maintenance of corneal transparency. *Trans Kans Acad Sci*. 1992;95:34-8.
11. Scott JE. Composition and structure of the pericellular environment. Physiological function and chemical composition of pericellular proteoglycan (an evolutionary view). *Philos Trans R Soc Lond B Biol Sci*. 1975;271:135-42.
12. Keene DR, Sakai LY, Lunstrum GP, Morris NP, Burgeson RE. Type VII collagen forms an extended network of anchoring fibrils. *J Cell Biol*. 1987;104:611-21.

13. Tisdale AS, Spurr-Michaud SJ, Rodrigues M, Hackett J, Krachmer J, Gipson IK. Development of the anchoring structures of the epithelium in rabbit and human fetal corneas. *Invest Ophthalmol Vis Sci*. 1988;29:727-36.

14. Haaskjold E, Refsum H, Refsum SB, Bjerknes R. Cell kinetics of the rat corneal epithelium. *Apmis*. 1992;100:1123-1128.

15. Lavker RM, Dong G, Cheng SZ, Kudoh K, Cotsarelis G, Sun TT. Relative proliferative rates of limbal and corneal epithelia. Implications of corneal epithelial migration, circadian rhythm, and suprabasally located DNA-synthesizing keratinocytes. *Invest Ophthalmol Vis Sci*. 1991;32:1864-1875.

16. Newsome DA, Foidart JM, Hassell JR, Krachmer JH, Rodrigues MM, Katz SI. Detection of specific collagen types in normal and keratoconus corneas. *Invest Ophthalmol Vis Sci*. 1981;20:738-50.

17. Jacobsen IE, Jensen OA, Prause JU. Structure and composition of Bowman's membrane. Study by frozen resin cracking. *Acta Ophthalmol (Copenh)*. 1984;62:39-53.

18. Lee RE, Davison PF. The collagens of the developing bovine cornea. *Exp Eye Res*. 1984;39:639-52.

19. Wilson MJ. Structure of the corneal stroma. *Vision Res*. 1970;10:519-20.

20. Meek KM, Blamires T, Elliott GF, Gyi TJ, Nave C. The organisation of collagen fibrils in the human corneal stroma: a synchrotron X-ray diffraction study. *Curr Eye Res*. 1987;6:841-6.

21. Newsome DA, Gross J, Hassell JR. Human corneal stroma contains three distinct collagens. *Invest Ophthalmol Vis Sci*. 1982;22:376-81.

22. Craig AS, Parry DA. Collagen fibrils of the vertebrate corneal stroma. *J Ultrastruct Res*. 1981;74:232-9.

23. Nakayasu K, Tanaka M, Konomi H, Hayashi T. Distribution of types I, II, III, IV and V collagen in normal and keratoconus corneas. *Ophthalmic Res*. 1986;18:1-10.

24. Scott JE, Haigh M. 'Small'-proteoglycan:collagen interactions: keratan sulphate proteoglycan associates with rabbit corneal collagen fibrils at the 'a' and 'c' bands. *Biosci Rep*. 1985;5:765-74.

25. Scott JE, Haigh M. Identification of specific binding sites for keratan sulphate proteoglycans and chondroitin-dermatan sulphate proteoglycans on collagen fibrils in cornea by the use of cupromeronic blue in 'critical-electrolyte-concentration' techniques. *Biochem J*. 1988;253:607-10.

26. Scott JE, Bosworth TR. A comparative biochemical and ultrastructural study of proteoglycan-collagen interactions in corneal stroma. Functional and metabolic implications. *Biochem J*. 1990;270:491-7.

27. Doane KJ, Babiarz JP, Fitch JM, Linsenmayer TF, Birk DE. Collagen fibril assembly by corneal fibroblasts in three-dimensional collagen gel cultures: small-diameter heterotypic fibrils are deposited in the absence of keratan sulfate proteoglycan. *Exp Cell Res*. 1992;202:113-24.

28. Mishima S. Clinical investigations on the corneal endothelium-XXXVIII Edward Jackson Memorial Lecture. *Am J Ophthalmol*. 1982;93:1-29.

29. Stur M, Grabner G. The corneal endothelium--morphology, function and clinical importance. *Wien Klin Wochenschr*. 1983;95:274-6.

30. Capella JA. Regeneration of endothelium in diseased and injured corneas. *Am J Ophthalmol*. 1972;74:810-7.

31. Renard G, Pouliquen Y, Hirsch M. Regeneration of the human corneal endothelium. *Albrecht Von Graefes Arch Klin Exp Ophthalmol*. 1981;215:341-8.

32. Hirsch M, Renard G, Faure JP, Payrau P. Proceedings: Regeneration of the rabbit corneal endothelium. A light and electron microscopic study. *Exp Eye Res*. 1975;20:182.

33. Hirsch M, Faure JP, Marquet O, Payrau P. Regeneration of corneal endothelium in the rabbit: microscopic study and relation with corneal thickness. *Arch Ophtalmol Rev Gen Ophtalmol*. 1975;35:269-78.

34. Schierholter R, Honegger H. Morphology of the corneal endothelium under normal conditions and during regeneration after mechanical injury. *Adv Ophthalmol*. 1975;31:34-99.

35. Axelsson I, Heinegard D. Fractionation of proteoglycans from bovine corneal stroma. *Biochem J*. 1975;145:491-500.

36. Coster L, Cintron C, Damle SP, Gregory JD. Proteoglycans of rabbit cornea: labelling in organ culture and in vivo. *Exp Eye Res*. 1983;36:517-30.

37. Scott JE, Cummings C, Greiling H, Stuhlsatz HW, Gregory JD, Damle SP. Examination of corneal proteoglycans and glycosaminoglycans by rotary shadowing and electron microscopy. *Int J Biol Macromol*. 1990;12:180-4.

38. Funderburgh JL, Conrad GW. Isoforms of corneal keratan sulfate proteoglycan. *J Biol Chem*. 1990;265:8297-303.

39. Funderburgh JL, Funderburgh ML, Mann MM, Conrad GW. Physical and biological properties of keratan sulphate proteoglycan. *Biochem Soc Trans*. 1991;19:871-6.

40. Greiling H. Structure and biological functions of keratan sulfate proteoglycans. *EXS*. 1994;70:101-22.

41. Asari A, Miyauchi S, Takahashi T, Kohno K, Uchiyama Y. Localization of hyaluronic acid, chondroitin sulfate, and CD44 in rabbit cornea. *Arch Histol Cytol*. 1992;55:503-11.

42. Nakamura M, Kimura S, Kobayashi M, Hirano K, Hoshino T, Awaya S. Type VI collagen bound to collagen fibrils by chondroitin/dermatan sulfate glycosaminoglycan in mouse corneal stroma. *Jpn J Ophthalmol*. 1997;41:71-6.

43. Rittig M, Lutjen-Drecoll E, Prehm P. Immunohistochemical localization of hyaluronan synthase in cornea and conjunctive of cynomolgus monkey. *Exp Eye Res*. 1992;54:455-60.

44. Lutjen-Drecoll E, Schenholm M, Tamm E, Tengblad A. Visualization of hyaluronic acid in the anterior segment of rabbit and monkey eyes. *Exp Eye Res*. 1990;51:55-63.

45. Madsen K, Schenholm M, Jahnke G, Tengblad A. Hyaluronate binding to intact corneas and cultured endothelial cells. *Invest Ophthal Vis Sci*. 1989;30:2132-7.

46. Härfstrand A, Molander N, Stenevi U, Apple P, Schenholm M, Madsen K. Evidence for hyaluronic acid binding sites on human corneal endothelium. *J Cataract Refract Surg*. 1992;18:265-9.

47. Fitzsimmons T, Fagerholm P, Härfstrand A, Schenholm M. Hyaluronic acid in the rabbit cornea after excimer laser superficial keratectomy. *Invest Ophthal Vis Sci*. 1992;33:3011-6.

48. Fagerholm P, Fitzsimmons T, Härfstrand A, Schenholm M. Reactive formation of hyaluronic acid in the rabbit corneal alkali burn. *Acta Ophthalmol (Copenh)*. 1992;70:67-72.

49. Molander N, Ehinger B, Rolfsen W, Härfstrand A, Stenevi U. Histochemical identification of hyaluronan in the rabbit anterior segment during the healing period after extracapsular lens extraction. *Acta Ophthalmol (Copenh)*. 1993;71:336-46.

50. Molander N, Lindquist U, Stenevi U, von Malmborg A, Ehinger B. Influence of radial keratectomy on endogenous hyaluronan in cornea and aqueous humour. *J Refractive & Corneal Surgery*. 1993;9:358-65.

51. Fitzsimmons TD, Molander N, Stenevi U, Fagerholm P, Schenholm M, von Malmborg A. Endogenous hyaluronan in corneal disease. *Invest Ophthalmol Vis Sci*. 1994;35:2774-82.

52. Funderburgh JL, Corpuz LM, Roth MR, Funderburgh ML, Tasheva ES, Conrad GW. Mimecan, the 25-kDa corneal keratan sulfate proteoglycan, is a product of the gene producing osteoglycin. *J Biol Chem*. 1997;272:28089-95.

53. Li W, Verges JP, Cornuet PK, Hassell JR. CDNA clone to chick corneal chondroitin/dermatan sulfate proteoglycan reveals identity to decorin. *Arch Biochem Biophys*. 1992;296:190-7.

54. Bianco P, Fisher LW, Young MF, Termine JD, Robey PG. Expression and localization of the two small proteoglycans biglycan and decorin in developing human skeletal and non-skeletal tissues. *J Histochem Cytochem*. 1990; 38:1549-63.

55. Funderburgh JL, Hevelone MR, Roth MR, Funderburgh ML, Rodrigues MR, Nirankari VS, Conrad GW. Decorin and biglycan of normal and pathologic human corneas. *Invest Ophthalmol Vis Sci*. 1998;39:1957-64.

56. Cintron C, Gregory JD, Damle SP, Kublin CL. Biochemical analyses of proteoglycans in rabbit corneal scars. *Invest Ophthalmol Vis Sci*. 1990;31:1975-81.

57. Funderburgh JL, Cintron C, Covington HI, Conrad GW. Immunoanalysis of keratan sulfate proteoglycan from corneal scars. *Invest Ophthalmol Vis Sci*. 1988;29:1116-24.

58. Forrester JV, Dick AD, McMenamin P, Lee WR. The eye. Basic sciences in practice. Chapter 4: Biochemistry. *London: W B Saunders Company LTD*, 1996.

59. Flaumenhaft R, Rifkin DB. The extracellular regulation of growth factor action. *Mol Biol Cell*. 1992;3:1057-1065.

60. Ruoslahti E, Yamagushi Y. Proteoglycans as modulators of growth factor activities. *Cell*. 1991;64:867-869.

61. Massagne J. A helping hand from proteoglycans. *Curr Biol*. 1991;2:117-119.

62. Alberts B, Bray D, Lewis J, Raff M, Roberts K, Watson JD. Molecular biology of the cell. Chapter 19: Cell junctions, cell adhesion, and the extracellular matrix. *New York & London: Garland Publishing Inc*, 1994.

63. Clark R, Henson P. The molecular and cellular biology of wound repair. *New York: Plenium Press*, 1988.

64. Philips AF, Szerenyi K, Campos M, Kreuger RR, McDonell PJ. Arachidonic acid metabolites after excimer laser corneal surgery. *Arch Ophthalmol*. 1993;111:1273-1278.

65. Gan L, Kim J, Fagerholm P. Effect of leukocytes on corneal cellular proliferation and wound healing. *Invest Ophthalmol Vis Sci*. 1999;40:575-81.

66. Kenyon K, Berman M, Rose J, Gage J. Prevention of stromal ulceration in the alkali-burned rabbit cornea by glue-on contact lens. Evidence for the role of polymorphonuclear leukocytes in collagen degradation. Invest Ophthalmol Vis Sci.1979;18:570-587.

67. Malecaze F, Simorre-Pinatel V, Chollet P, Tack JL, Muraine M, Le Guellec D, Vita N, Arne JL, Darbou JM. Interleukin-6 in the tear fluid after photorefractive keratectomy and its effects on keratocytes in culture. *Cornea*. 1997;16:580-587.

68. Grant M, Khaw P, Schultz G, Adam J, Shimizu R. Effect of epidermal growth factor, fibroblast growth factor and transforming growth factor on corneal cell chemotaxis. *Invest Ophthalmol Vis Sci*. 1992;33:3292-3301.

69. Schulz G, Khaw P, Oxford K, Macauley S, van Setten G, Chengi N. Growth factors and ocular wound healing. *Eye*. 1994;8:184-187.

70. Shah M, Foreman DM, Ferguson MW. Control of scarring in adult wounds by neutralising antibody to transforming growth factor beta. *Lancet*. 1992;339:213-214.

71. Myers J, Gomes J, Siepser S, Rapuano C, Eagle R, Thom S. Effect of transforming growth factor beta 1 on stromal haze following excimer laser photorefractive keratectomy in rabbits. *J Refract Surg*. 1997;13:356-361.

72. Tervo T, Vesaluoma M, Bennett G, Schwall R, Helena M, Liang Q, Wilson S. Tear hepatocyte growth factor (HGF) availability increases markedly after excimer laser surface ablation. *Exp Eye Res*. 1997;64:501-504.

73. Li Q, Tseng S. Differential regulation of cytokine and receptor transcript expression in human corneal and limbal fibroblasts by epidermal growth factor, transforming growth factor, platelet derived growth factor and interleukin-1beta. *Invest Ophthalmol Vis Sci*. 1996;37:727-739.

74. Sotozono C, Kinoshita S, Kita M, Imanishi. Paracrine role of keratinocyte growth factor in rabbit corneal epithelial cell growth. *Exp Eye Res*. 1994;59:385-392.

75. Kennedy M, Kim KH, Harten B, Brown J, Planck S, Meshul C, Edelhauser H, Rosenbaum JT, Armstrong CA, Ansel JC. Ultraviolet irradiation induces the production of multiple cytokines by human corneal cells. *Invest Ophthalmol Vis Sci*. 1997;38:2483-2491.

76. Crosson C, Klyce S, Beuerman R. Epithelial wound closure in the rabbit cornea: a biphasic process. *Invest Ophthalmol Vis Sci*. 1996;27:464-473.

77. Fujikawa L, Foster C, Lahigan J, Colvin R. Fibronectin in healing rabbit corneal wounds. *Lab Invest*.1981;45:120-129.

78. Khodadoust A, Silverstein A, Kenyon K, Dowling J. Adhesion and regenerating corneal epithelium. *Am J Ophthalmol*. 1968;79:65-69.

79. Hanna K, Pouliquen Y, Waring G, Savoldelli M, Fantes F, Thomson K. Corneal wound healing in monkeys after repeated excimer laser photorefractive keratectomy. *Arch Ophthalmol*. 1992;110:1286-1291.

80. Jester JV, Petroll WM, Barry P, Olsen DR, Cavanagh H. Inhibition of corneal fibrosis by topical application of blocking antibodies to TGFbeta in the rabbit. *Cornea*. 1997;16:177-187.

81. Poncelet A, Schnaper H. Regulation of human mesangial collagen expression by transforming growth factor-beta 1. *Am J Physiol*. 1998;275:458-466.

82. CIE. TC 6-26 report: Standardization of the Terms UV-A1, UV-A2, and UV-B. 1999;134/1.

83. Philips R. Sources and application of ultraviolet radiation. *London: Academic Press*,1983.

84. Dobson R. Exploring the atmosphere. Chapter 6: Ozone in the atmosphere. *Oxford: Claderon Press*, 1963.

85. Johnson FS, Mo T, Green AES. Average latitudinal variation in ultraviolet radiation at the Earth's surface. *Photochem Photobiol*. 1976;23:179-88.

86. Moan J, Dahlback A. The relationship between skin cancers, solar radiation and ozone depletion. *Br J Cancer*. 1992;65:916-21.

87. Nolan CV, Amanatidis GT. European Commission research on the fluxes and effects of environmental UVB radiation. *J Photochem Photobiol B*. 1995;31:3-7.

88. Munakata N. Continual increase in biologically effective dose of solar UV radiation determined by spore dosimetry from 1980 to 1993 in Tokyo. J Photochem Photobiol B. 1995;31:63-8.

89. Zeferos CS, Meleti C, Bais AF, Lambros A. The recent UVB variability over southeastern Europe. J Photochem Photobiol B. 1995;31:15-9.

90. Sliney D, Wollbarsht M. Optical hazards from the ambient environment. In: Sliney D, Wollbarsht M, ed. *Safety with lasers and other optical sources. A comprehensive handbook. New York: Plenum Press*, 1980:187-215.

91. Mellerio J. The design of effective ocular protection for solar radiation. In Sliney D, ed. *Measurments of optical radiation hazards. ICNIRP 6/98 and CIE x016-1998*, 1998:437-42.

92. Löfgren S. Cataract from ultraviolet radiation. *Stockholm: Karolinska University Press*, 2001.

93. Pitts D, Cameron LL, Jose JG. Optical radiation and cataracts. In: Waxler M, ed. *Optical radiation and visual health. Boca Raton: CRC Press*,1986:5-41.

94. Strzhizhovskii AD. The biomedical effects of ultraviolet radiation and their mechanisms. *Usp Fiziol Nauk*. 1995;26:98-112.

95. Longstreth J, de Gruijl FR, Kripke ML, Abseck S, Arnold F, Slaper HI, Velders G, Takizawa Y, van der Leun JC. Health risks. *J Photochem Photobiol B*. 1998;46:20-39.

96. Michael R. Development and repair of cataract induced by ultraviolet radiation. *Ophthalmic Res*. 2000;32 Suppl 1; 1-44.

97. Hamerski W, Zajaczkowska A. Electrophoretic investigations of proteins of the corneal epithelium in experimental photophthalmia. *Pol Med J*. 1969;8:1464-8.

98. Zigman S, Yulo T, Griess GA. Inactivation of catalase by near ultraviolet light and tryptophan photoproducts. *Mol Cell Biochem*. 1976;11:149-54.

99. Koliopoulos JX, Margaritis LH. Response of the cornea to far ultraviolet light: an ultrastructural study. *Ann Ophthalmol*. 1979;11:765-9.

100. Pitts DG, Cullen AP, Hacker PD. Ocular effects of near ultraviolet radiation: literature review. *Am J Optom Physiol Opt*. 1977;54:542-9.

101. Downes JE, Swann PG, Holmes RS. Ultraviolet light-induced pathology in the eye: associated changes in ocular aldehyde dehydrogenase and alcohol dehydrogenase activities. *Cornea*. 1993;13:241-8.

102. Foulks GN, Friend J, Thoft RA. Effects of ultraviolet radiation on corneal epithelial metabolism. *Invest Ophthalmol Vis Sci*. 1978;17:694-7.

103. Lattimore MR Jr. Effect of ultraviolet radiation on the energy metabolism of the corneal epithelium of the rabbit. *Photochem Photobiol*. 1989;49:175-80.

104. Bose B, Chatterjee SN. Correlation between UVA-induced changes in microviscosity, permeability and malondialdehyde formation in liposomal membrane. J Photochem Photobiol B. 1995;28:149-53.

105. Girotti AW. Photosensitized oxidation of membrane lipids: reaction pathways, cytotoxic effects, and cytoprotective mechanisms. *J Photochem Photobiol B*. 2001;63:103-13.

106. Wenk J, Brenneisen P, Meewes C, Wlaschek M, Peters T, Blaudschun R, Ma W, Kuhr L, Schneider L, Scharffetter-Kochanek K. UV-induced oxidative stress and photoaging. *Curr Probl Dermatol*. 2001;29:83-94.

107. Vega MP, Pizarro RA. Oxidative stress and defence mechanisms of the freshwater cladoceran Daphnia longispina exposed to UV radiation. *J Photochem Photobiol B*. 2000;54:121-5.

108. Limoli CL, Ward JF. Photochemical production of double-strand breaks in cellular DNA. *Mutagenesis*. 1995;10:453-6.

109. Kinley JS, Brunborg G, Moan J, Young AR. Detection of UVR-induced DNA damage in mouse epidermis in vivo using alkaline elution. *Photochem Photobiol*. 1995;61:149-58.

110. Schwalb G, Beyers AD, Anderson R, Nel AE. Promotion of DNA strand breaks in cocultured mononuclear leukocytes by protein kinase C-dependent prooxidative interactions of benoxaprofen, human polymorphonuclear leukocytes, and ultraviolet radiation. *Cancer Res*. 1988;48:3094-9.

111. Boullard A, Giacomoni PU. Effect of UV irradiation at defined wavelengths on the tertiary structure of double-stranded covalently closed circular DNA. *J Photochem Photobiol B*. 1988;2:491-501.

112. Estil S, Olsen WM, Huitfeldt HS, Haaskjold E. UVB-induced formation of (6-4) photoproducts in the rat corneal epithelium. *Acta Ophthalmol Scand*. 1997;75:120-3.

113. Chouinard N, Therrien JP, Mitchell DL, Robert M, Drouin R, Rouabhia M. Repeated exposures of human skin equivalent to low doses of ultraviolet-B radiation lead to changes in cellular functions and accumulation of cyclobutane pyrimidine dimers. *Biochem Cell Biol*. 2001;79:507-15.

114. Seidl H, Kreimer-Erlacher H, Back B, Soyer HP, Hofler G, Kerl H, Wolf P. Ultraviolet exposure as the main initiator of p53 mutations in basal cell carcinomas from psoralen and ultraviolet A-treated patients with psoriasis. *J Invest Dermatol*. 2001;117:365-70.

115. Krutmann J. Photocarcinogenesis. *Schweiz Rundsch Med Prax*. 2001;90:297-9.

116. Xu G, Marcusson JA, Hemminki K. DNA photodamage induced by UV phototherapy lamps and sunlamps in human skin in situ and its potential importance for skin cancer. *J Invest Dermatol*. 2001;116:194-5.

117. Mitchell J, Cenedella RJ. Quantitation of ultraviolet light-absorbing fractions of the cornea. *Cornea*. 1995;14:266-72.

118. Ringvold A. Cornea and ultraviolet radiation. *Acta Ophthalmol (Copenh)*. 1980;58:63-8.

119. Ringvold A. Corneal epithelium and UV-protection of the eye. *Acta Ophthalmol Scand*. 1998;76:149-53.

120. Cejkova J, Stipek S, Crkovska J, Ardan T. Changes of superoxide dismutase, catalase and glutathione peroxidase in the corneal epithelium after UVB rays. Histochemical and biochemical study. *Histol Histopathol*. 2000;15:1043-50.

121. Megaw JM. Glutathione and ocular photobiology. *Curr Eye Res*. 1984;3:83-7.

122. Hull DS, Riley MV, Csukas S, Green K. Corneal endothelial glutathione after photodynamic change. *Invest Ophthalmol Vis Sci*. 1982;22:405-8.

123. Ringvold A. In vitro evidence for UV-protection of the eye by the corneal epithelium mediated by the cytoplasmic protein, RNA, and ascorbate. *Acta Ophthalmol Scand*. 1997;75:496-8.

124. Ringvold A, Anderssen E, Kjonniksen I. Distribution of ascorbate in the anterior bovine eye. *Invest Ophthalmol Vis Sci*. 2000;41:20-3.

125. Reddy VN, Giblin FJ, Lin LR, Chakrapani B. The effect of aqueous humor ascorbate on ultraviolet-B-induced DNA damage in lens epithelium. *Invest Ophthalmol Vis Sci*. 1998;39:344-50.

126. Shimmura S, Suematsu M, Shimoyama M, Tsubota K, Oguchi Y, Ishimura Y. Subthreshold UV radiation-induced peroxide formation in cultured corneal epithelial cells: the protective effects of lactoferrin. *Exp Eye Res*. 1996;63:519-26.

127. Cejkova J, Lojda Z. The damaging effect of UV rays below 320 nm on the rabbit anterior eye segment. II. Enzyme histochemical changes and plasmin activity after prolonged irradiation. *Acta Histochem*. 1995;97:183-8.

128. Cejkova J, Lojda Z. The damaging effect of UV rays (with the wavelength shorter than 320 nm) on the rabbit anterior eye segment. I. Early changes and

their prevention by catalase-aprotinin application. *Acta Histochem*. 1994;96:281-6.

129. Pitts DG, Tredici TJ. The effects of ultraviolet on the eye. *Am Ind Hyg Assoc J*. 1971;32:235-46.
130. Pitts DG, Cullen AP, Hacker PD. Ocular effects of ultraviolet radiation from 295 to 365 nm. *Invest Ophthalmol Vis Sci*. 1977;16:932-9.
131. Kinsey VE. Spectral transmission of the eye to ultraviolet radiations. *Arch Ophthalmol (Chicago)*. 1948;39:508-13.
132. Boettner EA, Wolter JR. Transmission of ocular media. Invest Ophthalmol. 1962;1:776-83.
133. Zuclich JA, Kurtin WE. Oxygen dependence of near-ultraviolet induced corneal damage. *Photochem Photobiol*. 1977;25:133-5.
134. Widmark EJ. Ueber den Eifluss des Lichtes auf die vorderen Medien des Auges. *Scand Arch Physiol*. 1889;1:264.
135. Martin EK. The effects of ultra-violet rays upon the eye. *Proc Roy Soc (London)*. 1912;85:319.
136. Friedenwald JS, Buschke W, Crowell J, Hollaender A. Effects of ultraviolet irradiation on the corneal epithelium. *J Cell Comp Physiol*. 1948;32:161.
137. Moran DJ, Hollows FC. Pterygium and ultraviolet radiation: a positive correlation. *Br J Ophthalmol*. 1984;68:343-346.
138. Taylor HR. Aetiology of climatic droplet keratopathy and pterygium. *Br J Ophthalmol*. 1980;64:154-163.
139. Hill JC, Maske R. Pathogenesis of pterygium. *Eye*. 1989;3:218-26.
140. Levy WJ, Levy J, Clapper WE. Pterygium tissue culture histoimmunological study. *Arch Ophthalmol*. 1970;83:402-5.
141. Cameron ME. Histology of pterygium: an electron microscopic study. *Br J Ophthalmol*. 1983;67:604-8.
142. Klintworth GK. The cornea: structure and macromolecules in health and disease. *Am J Pathol*. 1977;89:717-808.
143. Clear AS, Chirambo MC, Hutt MSR. Solar keratosis, pterygium, and squamous cell carcinoma of the conjunctiva in Malawi. *Br J Ophthalmol*. 1979;63:102-109.

144. Dahan E, Judelson J, Welsh N. Regression of Labrador keratopathy following cataract extraction . *Br J Ophthalmol*. 1986;70:737-741.

145. Johnson GJ, Ghosh M. Labrador keratopathy: clinical and pathological findings. *Can J Ophthalmol*. 1975;10:119-135.

146. Johnson GJ, Overall M. Histology of spheroidal degeneration of the cornea in Labrador. *Br J Ophthalmol*. 1978;62: 53-61.

147. Wong WW. A hypothesis on the pathogenesis of pterygiums. *Ann Ophthalmol*. 1978;10:303-8.

148. Bietti GB, Guerra P, Ferraris de Gaspare PF. La dystrophie cornéenne nodulaire en ceinture des pays tropicaux a sol aride. Contributions cliniques et anatomo-pathologiqicue. *Bull Mem Soc Fr Ophtalmol*. 1955;68:101-29.

149. Falcone C. A tropical dystrophy. *East Afr Med J*. 1954;31:471-5.

150. Nataf R, Uveling N. Dystrophie cornéenne nodulaire en ceinture type Bietti. *Ann Ocul*. 1957;190:316-21.

151. Fretillere Y, Vedy J, Chovet M. A propos de 144 cas de dystrophie cornéenne de Bietti observés en Côte francaise des Somalis. *Med Trop*. 1967;27:293-302.

152. Roger FC. Clinical findings, course, and progress of Bietti's corneal degeneration in the Dahlak Islands. *Br J Ophthalmol*. 1973;57657-64.

153. Freedman A. Climatic droplet keratopathy. I. Clinical aspects. *Arch Ophthalmol*. 1973;89:193-7.

154. Anderson J, Fuglsang H. Droplet degeneration of the cornea in North Cameroon. Prevalence and clinical appearances. *Br J Ophthalmol*. 1976;60:256-62.

155. Vérin P, Farah T, Vildy A. Dystrophie nodulaire cornéenne ou dystrophie en ceinture de Bietti. *Rev Int Trach Pathol Ocul Trop Subtrop Sante Publique*. 1978;55:35-89.

156. Hanna C, Fraunfelder FT. Spheroidal degeneration of the cornea and conjunctiva. 2. Pathology. *Am J Ophthalmol*. 1972;74:829-39..

157. Garner A, Morgan G, Tripathi RC. Climatic droplet keratopathy. II. Pathologic findings. *Arch Ophthalmol*. 1973;89:198-204.

158. Jensen OA, Norn MS. Spheroid degeneration of the conjunctiva. Histochemical and ultrastuctural examination. *Acta Ophthalmol*. 1982;60:79-92.

159. Waring GO, Malaty A, Grossniklaus H, Kaj H. Climatic proteoglycan stromal keratopathy, a new corneal degeneration. *Am J Ophthalmol*. 1995;120: 330-341.

160. Pitts DG. A comparative study of the effects of ultraviolet radiation on the eye. *Am J Optom*. 1970;47:535-546.

161. Tengblad A. Affinity chromotography on immobilized hyaluronate and its application to the isolation of hyaluronate-binding proteins from cartilage. *Biochem Biophys Acta*. 1979;578:281-9.

162. Rippelino J, Klinger M, Margolis R. The hyaluronic acid binding region as a specific probe for the localisation of hyaluronic acid in tissue sectios: Application to chick embryo and rat brain. *J Histochem Cytochem.* 1985;33:1060-6.

163. Gavrieli Y, Sherman Y, Ben-Sasson SA. Identification of programmed cell death *in situ* via specific labeling of nuclear DNA fragmentation. *J Cell Biol.* 1992;119:493-501.

164. Kong J, Ringer DP. Quantitative *in situ* image analysis of apoptosis in well and poorly differentiated tumors from rat liver. *Am J Pathol.* 1995;147:1626-1632.

165. Liu Q, Oshima K, Shinohara T, Kikuchi M. Apoptosis in histiocytic necrotizing lymphadenitis. *Pathology International.* 1995;45:729-734.

166. Su JH, Anderson AJ, Cummings BJ, Cotman CW. Immunohistochemical evidence for apoptosis in Alzheimer`s disease. *Neuroreport*. 1994;5:2529-2533.

167. Hellio le Graverand MP, Reno C, Hart DA. Gene expression in menisci from the knees of skeletally immature and mature female rabbits. *J Orthop Res*. 1999;17:738-44.

168. Applequist SE, Keyna U, Calvin MR, Beck-Engeser GB, Raman C, Jack HM. Sequence of the rabbit glyceraldehyde-3-phosphate dehydrogenase-encoding cDNA. *Gene*. 1995;163:325-6.

169. Pitts DG. A comparative study of the effects of ultraviolet radiation on the eye. *Am J Optom*. 1970;47:535-46.

170. Pitts DG, Prince JE, Butcher WI, et al. The effects of ultraviolet radiation on the eye. *USAF Scool of Aerospace Medicine, Brooks Air Force Base, Texas, 1969, Monograph No SAM-TR-69-10.*

171. Sherashov SG. Spectral sensitivity of the cornea to ultraviolet rediation. *Biofizika*. 1970;15:543-4.

172. Ringvold A, Davanger M. Changes in the rabbit corneal stroma caused by UV radiation. *Acta Ophthal (Copenh).* 1985;63:601-6.

173. Ringvold A. Damage of the cornea epithelium caused by ultraviolet radiation. A scanning electron microscopic study in rabbit. *Acta Ophthalmol (Copenh).* 1983;61:898-907.

174. Ringvold A, Davanger M, Olsen EG. Changes of the cornea endothelium after ultraviolet radiation. *Acta Ophthalmol (Copenh).* 1982;60:41-53.

175. Pitts DG, Chu LW-F, Brgemanson JPG, Jose JG, Waxler M, Hitchins VM. Damage and recovery in the UV-exposed cornea. In: Cronly-Dillon, J Rosen & ES Marshall, eds. *Hazards of Light, Myths and Realities. Eye and skin.* Pergamon Press, Oxford, pp 209-219, 1986.

176. Campos M, Szerenyi K, Lee M, McDonnell J, McDonnell P. Keratocyte loss after corneal de-epithelialization in primates and rabbits. *Arch Ophthalmol.* 1994;112:254-60.

177. Wilson SE, He Y-G, Weng J et al. Epithelial injury induces keratocyte apoptosis: Hypothesized role for the interleukin-1 system in the modulation of corneal tissue organization and wound healing. *Exp Eye Res.* 1996;62:325-7.

178. Cohen JJ. Apoptosis: Physiological cell death. *J Lab Clin Med.* 1994;124:761-65.

179. Thompson CB. Apoptosis in the pathogenesis and treatment of disease. *Science.* 1995;267:1456-62.

180. Arends MJ, Wyllie AH. Apoptosis: mechanisms and roles in pathology. *Int Rev Pathol.* 1991;32:223-54.

181. Wyllie AH, Kerr JFR, Currie AR. Cell death: The significance of apoptosis. *Int Rev Cytol.* 1980;68:251-306.

182. Bowen ID, Bowen SM. Programmed cell death in tumors and tissues. New York: Chapman & Hall, 1990.

183. Tomei LD, Cope FO. Apoptosis: The molecular basis of cell death. In: Inglis J, Witkowski JA, eds. Current Communications in Cell & Molecular Biology. Vol. III. Cold Spring Harbor, New York: Cold Spring Harbor Laboratory Press;1991.

184. Bursch W, Kleine L. The biochemistry of cell death by apoptosis. *Biochem Cell Biol.* 1990;68:1071-4.

185. Fesus L, Davies PA, Piacenti M. Apoptosis: Molecular mechanisms in programmed cell death. *Eur J Cell Biol.* 1991;56:170-77.

186. Ren H, Wilson G. Apoptosis in the corneal epithelium. *Invest Ophthalmol Vis Sci.* 1996;37:1017-25.

187. Glaso M, Sandvig KU, Haaskjold E. Apoptosis in the rat corneal epithelium during regeneration. A transmission electron microscopic study. *APMIS.* 1993;101:914-22.

188. Levi H, Nielsen A. An autoradiographic study of cell kinetics on epidermis of the toad, *Bufo bufo. J Invest Dermatol.* 1982;79:292-6.

189. Budtz PE. Epidermal tissue homeostasis I: Cell pool size, cell birth rate and cell loss by moulting in the intact toad, *Bufo bufo. Cell Tissue Kinet.* 1985;18:521-32.

190. Clark SM, Doughty MJ, Cullen AP. Acute effects of ultraviolet-B irradiation on the corneal surface of the pigmented rabbit studied by quantitative scanning electron microscopy. *Acta Ophthalmol (Copenh).* 1990;68:639-50.

191. Helena MC, Baerveldt F, Kim W-J, Wilson SE. Keratocyte apoptosis following corneal surgery. *Invest Ophthalmol Vis Sci.* 1998;39:276-83.

192. Ishizaki M, Arar H, Wander AH, Kao WWY. Apoptosis during corneal wound-healing. [ARVO abstract]. *Invest Ophthalmol Vis Sci.* 1995;36:S865.

193. Wilson SE, Pedroza L, Beuerman R, Hill JM. Herpes simplex virus type-1 infection of corneal epithelial cells induces apoptosis of the underlying keratocytes. *Exp Eye Res.* 1997;64:775-9.

194. Wilson SE. Programmed cell death, wound healing, and laser refractive surgical procedures: molecular-cell biology for the corneal surgeon. *J Refract Surg.* 1997;13:171-5.

195. Wilson SE, Li Q, Weng J, Barry-Lane PA, Jester JV, Liang Q, Wordinger RJ. The Fas/Fas Ligand system and other modulators of apoptosis in the cornea. *Invest Ophthalmol Vis Sci* 1996;37:1582-92.

196. Griffith TS, Brunner T, Fletcher SM, Green DR, Ferguson TA. Fas ligand-induced apoptosis as a mechanism of immune privilege. *Science* 1995;270:1189-92.

197. Nagata S, Golstein P. The Fas death factor. *Science* 1995;267:1449-56.

198. Itoh N, Yonehara S, Ishii A, Yonehara M, Mizushima S, Sameshima M, Hase A, Seto Y, Nagata S. The polypeptide encoded by the cDNA for human cell surface antigen Fas can mediate apoptosis. *Cell* 1991;66:233-43.

199. Trauth BC, Klas C, Peters AMJ, Matzku S, Moeller P, Falk W, Debatin KM, Krammer PH. Monoclonal antibody-mediated tumor regression by induction of apoptosis. *Science* 1989;245:301-5.

200. Cheng J, Liu C, Koopman WJ, Mountz JD. Characterization of human Fas gene: Exon/intron organization and promoter region. *J Immunol* 1995;154:1239-45.

201. Alderson M. Fas ligand mediates activation induced cell death in human T lymphocytes. *J Exp Med* 1995;181:71.

202. Takahashi T, Tanaka M, Inazawa J, Abe T, Suda T, Nagata S. Human Fas ligand: Gene structure, chromosomal location and species specificity. *Int Immunol* 1994;6:1567-74.

203. Tanaka M, Suda T, Takahashi T, Nagata S. Expression of the functional soluble form of human fas ligand in activated lymphocytes. *EMBO J* 1995;14:1129-35.

204. Kimura K, Wakatsuki T, Yamamoto M. A variant mRNA species encoding a truncated form of Fas antigen in the rat liver. *Biochem Biophys Res Commun* 1994;198:666-74.

205. Mohan RR, Liang Q, Kim WJ, Helena MC, Baerveldt F, Wilson SE. Apoptosis in the cornea: Further characterization of Fas/Fas ligand system. *Exp Eye Res* 1997;65:575-89.

206. Cheng J, Zhou T, Liu C, Shapiro JP, Brauer MJ, Kiefer MC, Barr PJ, Mountz JD. Protection from Fas-mediated apoptosis by a soluble form of the Fas molecule. *Science* 1994;263:1759-62.

207. Liu C, Cheng J, Mountz JD. Differential expression of human Fas mRNA species upon peripheral blood mononuclear cell activation. *Biochem J* 1995;310:957-63.

208. Cascino I, Fiucci G, Papoff G, Ruberti G. Three functional soluble forms of the human apoptosis-inducing Fas molecule are produced by alternative splicing. *J Immunol* 1995;154:2706-13.

209. Papoff G, Cascino I, Eramo A, Starace G, Lynch DH, Ruberti G. An N-terminal domain shared by Fas/Apo1 (CD95) soluble variants prevents cell death in vitro. *J Immunol* 1996;156:4622-30.

210. Laurent TC. Structure of hyaluronic acid. In: Balazs EA, ed. *Chemistry and Molecular Biology of the Intercellular Matrix*. London; 1970:703.

211. Comper WD, Laurent TC. Physiological function of connective tissue polysaccharides. *Physiol Rev*. 1978;58:255-315.

212. Lindahl U, Hook M. Glycosaminoglycans and their binding to biological macromolecules. *Ann Rev Biochem*. 1978;47:385-417.

213. Maroudas A, Weinberg PD, Parker KH, Winlove CP. The distribution and diffusivities of small ions in chondroitin sulphate, hyaluronate and some proteoglycan solutions. *Biophys Chem*. 1988;32:257-70.

214. Parker KH, Winlove PD, Maroudas A. The theoretical distributions and diffusivities of small ions in chondroitin sulphate and hyluronate. *Biophys Chem*. 1988;32:271-82.

215. Yue B, Baum J, Silbert J. The synthesis of glycosaminoglycans by cultures of corneal stromal cells from patients with keratoconus. *J Clin Invest*. 1979;63:545-51.

216. Yue B, Baum J, Silbert J. Synthesis of glycosaminoglycans by cultures of normal human corneal endothelial and stromal cells. *Invest Ophthal Vis Sci*. 1978;17:523-7.

217. Dahl I, Cöster L. Proteoglycans biosynthesis in cultures of corneas and cornea stroma cells from adult rabbit. *Exp Eye Res*. 1978;27:175-90.

218. Dahl I, Johnsen W, Anseth P, Prydz H. The synthesis of proteoglycans by corneal stroma cells in culture. *Exp Cell Res*. 1974;88:193-7.

219. Dahl I. Biosynthesis of proteoglycans and hyaluronate in rabbit corneal fibroblast cultures. Variation with age of the cell line and effect of foetal calf serum. *Exp Eye Res.* 1981;32:419.

220. Conrad G, Hamilton C, Haynes E. Differences in glycosaminoglycans synthesized by fibroblast-like cells from cornea, heart, and skin. *J Biol Chem.* 1977;252:6861-70.

221. Madsen K, Schenholm M, Jahnke G, Tengblad A. Hyaluronate binding to intact corneas and cultured endothelial cells. *Invest Ophthal Vis Sci.* 1989;30:2132-7.

222. Wong YK, Tang KT, Wu JC, Hwang JJ, Wang HS. Stimulation of hyaluronan synthesis by interleukin-1beta involves activation of protein kinase C betaII in fibroblasts from patients with Graves' ophthalmopathy. *J Cell Biochem.* 2001;82:58-67.

223. Matsumoto J, Yanagisawa N, Konoma T, Hairuka H, Nakashima Y, Sato M. Increased Fas antigen in uremia accelerates adhesion of mononuclear cells to endothelial and sinovial cells via stimulated hyaluronan production. *Am J Kidney Dis*. 2001;38(4 Suppl 1):S54-7.

224. Usui T, Amano S, Oshika T, Suzuki K, Miyata K, Araie M, Heldin P, Yamashita H. Expression regulation of hyaluronan sythase in corneal endothelial cells. *Invest Ophthalmol Vis Sci*. 2000;41:3261-7.

225. Toole B, Trelstad R. Hyaluronate production and removal during corneal development in the chick. *Dev Biol*. 1971;26:28-35.

226. Hart G. Biosynthesis of glycosaminoglycans by the separated tissues of the embryonic chick cornea. *Dev Biol*. 1978;62:78-98.

227. Trelstad R, Hayashi K, Toole B. Epithelial collagens and glycosaminoglycans in the embryonic cornea. *J Cell Biol*. 1974;62:815-30.

228. Miyaushi S, Sugiyama T, Machida et al. The effects of sodium hyaluronate on the migration of rabbit corneal epithelium. I. An in vitro study. *J Ocul Pharmacol*. 1990;6:91-9.

229. Nishida T, Nakamura M, Mishima H, Otori T. Hyaluronan stimulates corneal epithelial migration. *Exp Eye Res.* 1991;53:753-8.

230. Tammi R, Tammi M. Correlations between hyaluronan and epidermal proliferation as studied by [3H]glucosamine and [3H]thymidine incorporations and staining of hyaluronan on mitotic keratinocytes. *Exp Cell Res*. 1991;195:524-7.

231. Inoue M, Katakami C. The effects of hyaluronic acid on corneal epithelial cell proliferation. *Invest Ophthal Vis Sci*. 1993;34:2313-5.

232. Longaker MT, Chiu ES, Adzick NS, Stern M, Harrison MR, Stern R. Studies in fetal wound healing. V. A prolonged presence of hyaluronic acid characterizes fetal wound fluid. *Ann Surg*. 1991;213:292-6.

233. Laurent U, Dahl L, Lilja K. Hyaluronan injected in the anterior chamber of the eye is catabolized in the liver. *Exp Eye Res*. 1993;57:435-440.

234. Culty M, Nguyen HA, Underhill CB. The hyaluronan receptor (CD44) participates in the uptake and degradation of hyaluronan. *J Cell Biol*. 1992;11:1055-1062.

235. Asari A, Miyauchi S, Takahashi T, Kohno K, Uchiyama Y. Localization of hyaluronic acid, chondroitin sulphate, and CD44 in rabbit cornea. *Arch Histol Cytol*.1992;55:503-511.

236. Schwartz DM, Jumper MD, Dang S, Schuster S, Stern R. Corneal endothelial hyaluronidase: a role in anterior chamber hyaluronic catabolism. *Cornea*. 1997;16:188-191.

237. Kim W-J, Helena MC, Mohan RR, Wilson SE. Changes in corneal morphology associated with chronic epithelial injury. *Invest Ophthalmol Vis Sci*. 1999;40: 35-42.

238. Fraser JRE, Laurent TC. Turnover and metabolism of hyaluronan. In: Evered D and Whelan J ed. *The Biology of Hyaluronan.* Chichester: John Wiley. 1989: 41-56.

239. Rolfsen W, Holst A, Lundgren B, Svensson B. The initiation of free radicals during phacoemulsification. *Invest Ophthalmol Vis Sci*. 1993;34: 1453.

240. Shimmura S, Masumizu T, Nakai Y, Urayama K, Shimazaki J, Bissen-Miyajima H, Kohno M, Tsubota K. Excimer laser-induced hydroxyl radical formation and keratocyte death in vitro. *Invest Ophthalmol Vis Sci*. 1999;40: 1245-1249.

241. Cai L, Cheridan MG. Adaptive response to ionizing radiation-induced chromosome aberrations in rabbit lymphocytes: effect of pre-exposure to zinc, and copper salts. *Mutat Res.* 1996;369: 233-241.

242. Cai L, Satoh M, Tohyama C, Cherian MG. Metallothionein in radiation exposure: its induction and protective role. *Toxicology*. 1999;132: 85-98.

243. Dudek EJ, Peak JG, Roth RM, Peak MJ. Isolation of V79 fibroblast cell lines containing elevated metallothionein levels that have increased resistance to the cytotoxic effects of ultraviolet-A radiation. *Photochem Photobiol*. 1993;58: 836-840.

244. Funderburgh JL, Funderburgh ML, Mann MM, Corpuz LM, Roth MR. Proteoglycan expression during transforming growth factor beta-induced keratocyte-myofibroblast transdifferentiation. *J Biol Chem*. 2001 Sept 12; [epub ahead of print].

245. Roughley PJ, Rodriguez E, Lee ER. The interactions of `non-aggregating` proteoglycans. *Osteoarthritis Cartilage*. 1995;3:239-48.

8. APPENDICES